Deep–Sea Research I 221 (2025) 104513

Contents lists available at ScienceDirect

Deep-Sea Research Part I

journal homepage: www.elsevier.com/locate/dsri

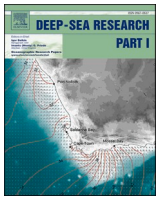

Creepy-Crawlies of the Arctic deep sea: Metazoan meiobenthic communities across latitudinal and bathymetric gradients in the western Arctic Ocean

Jona R. Silberberg [a,*], Dieter Piepenburg [b,c], Christiane Hasemann [a]

[a] Helmholtz Gemeinschaft – Max Planck Gesellschaft Joint Research Group for Deep-Sea Ecology and Technology, Alfred Wegener Institute Helmholtz-Centre for Polar and Marine Research, Bremerhaven, Germany
[b] Alfred Wegener Institute, Helmholtz Centre for Polar and Marine Research, Bremerhaven, 27570, Germany
[c] Institute for Ecosystem Research, Christian Albrechts University of Kiel, Kiel, 24118, Germany

ARTICLE INFO

Keywords:
Meiobenthic communities
Deep sea
Central Arctic
Bathymetric transect

ABSTRACT

Knowledge on meiofauna in the Arctic Ocean is lacking despite their importance for ecosystem functioning. The Synoptic Arctic Survey aimed to fill such knowledge gaps and thus included meiofaunal sampling. A bathymetric transect (from shelf to central basins) was sampled in the western Arctic Ocean during the HLY2202 expedition. Four sampled transect stations were investigated to answer three key questions: (1) How does the meiofaunal community change along the transect? (2) Which sedimentary parameters drive the meiofaunal community compositions? (3) Has the meiofaunal community at the North Pole changed since 1996, and if so, how? The uppermost 3 cm of sediment were analyzed for metazoan meiofaunal composition (including meiofaunal abundance and nematode biomass) in relation to food proxies (i.e. bacterial abundance and biomass, organic carbon, phospholipids, chlorophyll *a*, phaeophytin) and sediment porosity. Meiofaunal density and taxa count decreased with increasing water and sediment depth, as did nematode body sizes. This supported the concept of deep-sea miniaturization. Thicker nematodes dominated near-surface sediments, while slimmer individuals dominated deeper layers, a pattern related to sediment porosity. Sediment pigments (i.e. chlorophyll) and bacteria were confirmed as important food sources, and sediment porosity was corroborated as an important driver of meiofaunal communities. Virtually no differences were found in abundance of higher meiofauna taxa at the North Pole between 1996 and 2022, potentially due to relative stability provided by the still permanent ice-cover. Examining the meiofaunal composition at genus level will allow analysis of potential changes in diversity and ecosystem functions in relation to environmental changes.

1. Introduction

The deep sea has been a source of fascination and mystery for centuries. Early assumptions of uninhabitable, dead abyssal plains, such as Forbes' "azoic hypothesis" (Forbes and Reeve, 1855), have long been discredited, as has the concept of a "homogenous" deep-sea desert (see Anderson and Rice, 2006). Biogenic structures and *Lebensspuren* (Przeslawski, 2020) on the deep-sea floor, such as polychaete mud balls or agglutinated foraminiferan tests, provide ample evidence of a heterogenous environment teeming with life (Coull, 1988; Thistle, 1978).

Meiofauna, defined as the fraction of organisms passing through a 500-μm sieve but retained by a 44-μm sieve (although a 32-μm sieve is often used in deep-sea studies) (Giere, 2009; Giere and Schratzberger, 2023), play a crucial role in deep-sea ecosystems and their functions. Gerlach (1971) outlines that for an equivalent biomass, meiofaunal metabolism is five times that of larger macrofaunal organisms. In the deep sea, the ratio of macrofaunal to meiofaunal biomass is estimated to be approximately one (Gerlach, 1971), meaning that meiofauna are the key players in benthic energetics in deep-sea systems (Coull, 1988).

Meiofaunal organisms perform essential ecosystem functions in sediments, including provisioning, regulating, maintaining and enriching processes (Rosli et al., 2018; Schratzberger and Ingels, 2018). They play a key role in benthic food webs, consuming lower trophic levels (e.g. bacteria) and being consumed by higher trophic levels (e.g. fish, shrimp). Meiofauna also stimulate microbial communities through the excretion of extracellular polymeric substances (EPS) and bioturbated

* Corresponding author.
E-mail address: jonasilberberg@gmail.com (J.R. Silberberg).

https://doi.org/10.1016/j.dsr.2025.104513
Received 28 January 2025; Received in revised form 23 April 2025; Accepted 1 May 2025
Available online 2 May 2025

sediments, enhancing nutrient exchange and detritus remineralization (Coull, 1988; Heip et al., 1985; Rosli et al., 2018).

Investigating the composition of meiofaunal communities is essential for understanding these ecosystem functions. Previous studies have identified various environmental gradients, particularly water depth, as key drivers of meiofaunal distributions (Rosli et al., 2018; Soltwedel, 2000; Thiel, 1983; Tietjen, 1992). Benthic abundance typically decreases with depth, mainly due to reduced food availability as organic matter from surface primary production decreases during descent (Alldredge and Silver, 1988; Azam and Malfatti, 2007; Grebmeier and Barry, 1991). Parameters such as organic carbon, phospholipids, and sediment parameters (e.g. porosity, grain size) are used to study these gradients (Schnier et al., 2023; Soltwedel et al., 2016, 2020).

In polar regions, deep-sea food supply is further affected by sea ice, which influences primary production and carbon flux to the seafloor (Ingels et al., 2023a). Arctic meiofaunal gradients are influenced by ice cover, distance from shelves, and water depth (Renaud et al., 2006; Vanreusel et al., 2000). Arctic sea ice has been significantly affected by global climate change, altering marine primary production, as well as food availability in sympagic, pelagic and benthic ecosystems (Constable et al., 2022; Grebmeier, 2012; Grebmeier et al., 2006; Piepenburg, 2005).

Since the first quantitative deep-sea meiofauna study (Wigley and McIntyre, 1964), research of meiofauna has become widespread. However, investigations have largely been focused on continental margins while deep-sea basins remain understudied, particularly in polar regions (Rosli et al., 2018). This is mainly due to the significant logistical, technical and financial challenges related to sampling in these environments. A prominent example of Arctic continental margin research is the meiobenthic time-series investigation (e.g., Hasemann et al., 2020; Soltwedel et al., 2018, 2020) conducted at the long-term ecological research observatory HAUSGARTEN in the Fram Strait between Greenland and Svalbard, established by the Alfred Wegener Institute for Polar and Marine Research in 1999 (Soltwedel et al., 2005, 2016). The sampling and processing methodology of these investigations is used as a guideline for the present study. For a summary of further Arctic meiofaunal studies see Ingels et al. (2023a).

In the deep-sea basins of the central Arctic Ocean, however, rather few studies have examined meiofaunal communities (see e.g. Vanreusel et al. (2000) and Renaud et al. (2006)). Schewe and Soltwedel (1999) conducted a study on deep-sea meiobenthic communities in deep-sea basins and along submarine ridges, including a station at the North Pole (90°N), during the "Arctic Ocean '96" cruise aboard Swedish icebreaker ODEN. Since these samples were collected in 1996, the seasonal minimum sea-ice extent of the Arctic in the month of September has reduced from 6.75 million to 4.67 million square kilometers in 2022 ("NASA Scientific Visualization Studio | Annual Arctic Sea Ice Minimum, 1979–2015 with Area Graph," 2016; National Snow and Ice Data Center, 2022).

Thus, as established, there is a research gap regarding meiofaunal studies in the central Arctic Ocean, a region which has been changing markedly in the past decades. Filling such research gaps in Arctic research was the aim of the Synoptic Arctic Survey (SAS). SAS took a pan-Arctic interdisciplinary approach to answer this overarching key question: What are the present state and major ongoing transformations of the Arctic marine system (Paasche et al., 2019)? The US-American contribution to the SAS comprised a sampling campaign of the western Arctic Ocean, which included the sampling of benthic meiofauna.

The main objective of the present study is to examine the metazoan meiobenthic samples collected during the US American SAS cruise, which explored a bathymetric/latitudinal transect across the Amerasian basin to the North Pole. The sampled meiobenthic communities will be studied in relation to ambient sedimentary background sedimentary parameters (i.e. food proxies and sediment porosity). At the North Pole station, the community composition is compared to data published by Schewe and Soltwedel (1999) to evaluate community change between 1996 and 2022. This leads to the formulation of the following research questions:

1. How does the metazoan meiofauna community composition (with special focus on nematode body form and biomass) change along a bathymetric/latitudinal transect from 1700 m to 4300 m depth and 77° to 90°N in the western Arctic?
2. What environmental factors influence meiofaunal community patterns? Do certain factors have a comparatively greater influence than others?
3. Are there any changes in the meiofaunal community composition sampled at the North Pole in 1996 and 2022 (present study)?

2. Materials and methods

2.1. Study site

Sampling was conducted during the HLY2202 cruise (September 4th to October 24th, 2022) aboard the US-American icebreaker USCGC Healy (Ashjian and Grebmeier, 2024). For this study, four stations along a latitudinal and water-depth transect in the western Arctic Ocean were selected. Latitudes ranged from 77°N to 90°N and water depth ranged from 1720 m to 4237 m depth (Fig. 1, Table 1).

The sampling transect covered two major deep-sea basins and one ridge in the western Arctic Ocean: stations 31 and 27 are located on the Mendeleev Ridge, station 22 in the Makarov Basin, and station 21 (North Pole station) beyond the Lomonosov Ridge in the Amundsen Basin. These are impacted by different water inflows to the Arctic (see Rudels and Carmack, 2022).

2.2. Sediment sampling

Sediment samples were collected by an 8-tube Multi-Core 800 (multiple corer, MUC). MUC cores, with an inner diameter of 9.5 cm, were subsampled for meiofauna and an array of biogeochemical and physical background sedimentary parameters (bacterial abundance and biomass, organic carbon (C-org), phospholipids (LIPID), chloroplastic pigment equivalents (CPE), and water content (%H2O)). Subsampling was conducted by means of plastic syringes with cut-off ends, essentially acting as small piston-corers (Fleeger et al., 1988).

Depending on the parameters sampled, 1.2 cm (bacteria, organic carbon, chloroplastic pigment equivalents) and 2.0 cm (meiofauna, phospholipids, water content) diameter syringes were used to subsample the top 5 cm of sediment. For each of the parameters, three pseudo-replicates, each from a different MUC core, were collected at all stations, except bacteria, for which only one sediment replicate was collected at all stations. For certain parameters fewer viable replicates were evaluated due to logistical constraints (Table A.1).

2.3. Sample processing

Sample processing for this study was based on the methodology of the meiofaunal studies conducted at the HAUSGARTEN observatory (Soltwedel et al., 2005).

2.3.1. Meiofauna

After sampling, the sediment samples for meiofauna were sectioned into 1-cm layers (i.e., 0–1 cm, 1–2 cm, 2–3 cm, 3–4 cm, 4–5 cm), fixed in a 4 % formaldehyde/filtered-seawater solution and stored until analyzed in the laboratory. For meiofauna extraction, the samples were washed over a 32-µm mesh sieve to remove the formaldehyde. As described in Heip et al. (1985) and Vincx (1996), the fraction remaining on the sieve was re-suspended and centrifuged in solution of colloidal silica LUDOX TS50 (diluted at a specific gravity of 1.18 g cm^{-3}). After centrifugation, the supernatant containing the organisms was decanted and rinsed over a 32 µm-mesh sieve to remove remaining Ludox. This

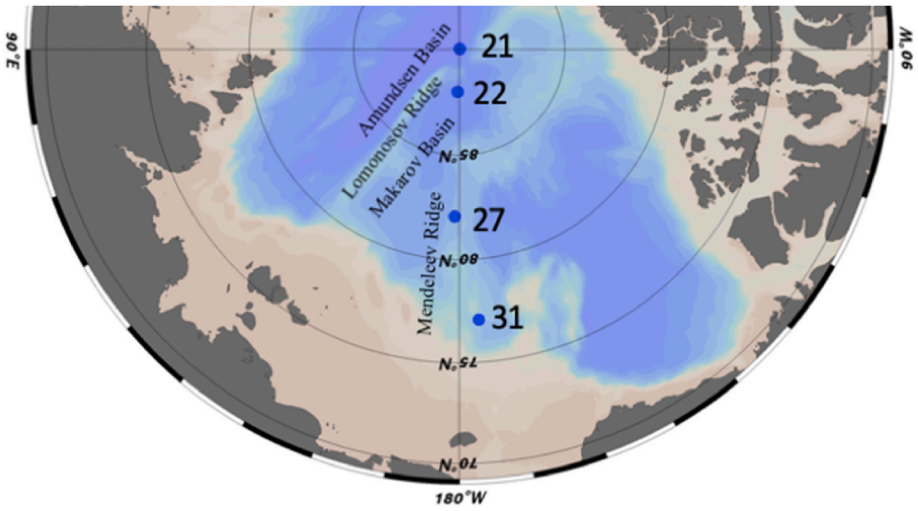

Fig. 1. Map indicating geographic locations of the four multiple-corer sampling stations along the latitudinal bathymetric transect performed during HLY2202 cruise aboard the US-American icebreaker USCGC Healy between September 4th, 2022 and October 24th, 2022. Sea-ice coverage was variable along the transect. In 2022, stations 21, 22, and 27 were permanently ice-covered, while station 31 was not ice-covered during summer (National Snow and Ice Data Center (NSIDC), 2022).

Table 1
Multiple-corer sampling stations, dates, geographic locations and water depths during HLY2202 cruise aboard the US-American icebreaker USCGC Healy between September 4th, 2022 and October 24th, 2022.

Station	mm/dd/yy hh:mm	Latitude °N	Longitude °E	Depth (m)
21	10/02/22 02:48	89.974	−53.445	4237
22	10/05/22 06:42	87.976	177.819	3943
27	10/11/22 04:08	82.070	178.501	2358
31	10/15/22 03:22	77.083	−175.832	1720

process was repeated twice to maximize the number of extracted organisms. Meiofaunal organisms were subsequently transferred to a petri dish and stained with Rose Bengal to facilitate the identification of organisms within the remaining sediment. All metazoan organisms were counted and classified at higher taxonomical groups (here: Nematoda, Harpacticoida, Cnidaria, Polychaeta, Nauplii, Kinorhyncha, Annelida, Ostracoda, and Loricifera) using an OLYMPUS SZX16 stereomicroscope. Following the processing and evaluating of the first sediment sample, in which a very strong decrease in meiofaunal density with increasing sediment depth was noted – virtually no organisms were present in layers 4 and 5 – only the top 3 cm were evaluated for the remaining samples.

2.3.2. Nematode biomass

Nematodes were handpicked from the petri dishes and mounted as permanent slides with anhydrous glycerin. A paraffin wax seal secured the nematodes between the slide and the cover glass. Prior to mounting, to prevent tissue damage and shrinkage due to abrupt changes in osmolarity, handpicked nematodes were kept in a solution of water, ethanol and glycerin in a desiccator cabinet until water and ethanol evaporated, leaving the pure glycerin (Seinhorst, 1959, 1962).

The prepared slides were examined under an OLYMPUS BX53 light microscope equipped with an OLYMPUS DP28 digital camera. The length (excluding filiform tails) and maximum width were measured using the polygon-measurement-tool in the cellSens Entry v3.2 software. The biomass was subsequently calculated from the length and width data with the Andrássy (1956) formula: $WW = (L*W^2)/Cf$, with:

WW [µg] = *wet weight*

L [µm] = *nematode's length*

W [µm] = *nematode's width at widest point*

Cf = *conversion factor which equals 1.6 * 10^6*.

The dry weight of the nematodes, which was used throughout biomass analyses, was calculated by using the dry-to wet-weight ratio of 0.25 (Wieser, 1960).

2.3.3. Background sedimentary parameters: food proxies and porosity

The bacterial sediment samples were sectioned into 1 cm layers, fixed in a 4 % formaldehyde solution, and stored for later laboratory analysis. There, bacteria were separated from the sediment by ultrasound and diluted to a concentration of 1:4000 with a 4 % filtered-seawater/formaldehyde solution. After staining the samples with acridine orange solution, bacterial cells in 40 different visual fields were counted by epifluorescence microscopy (see Meyer-Reil, 1983) to determine the total bacterial number (TBN). A Porton grid was used to determine bacterial volume (Grossmann and Reichardt, 1991). Length and width of 50 randomly selected bacteria, measured with an eyepiece graticule, was used to determine the biomass per cell, which was estimated using a conversion factor of 3.0×10^{-13} g C μm^{-3} (Børsheim et al., 1990).

After sampling, the sediment samples for C-org, LIPID, CPE, and % H2O were shock-frozen at −80 °C and stored at −20 °C until analyzed in the laboratory. Total organic carbon content (C-org) of the sediments was determined with an Eltra CS 800 elemental analyzer. Phospholipids, as key components of cell membranes, can be used to determine the viable membrane biomass of all microbes, that is the total microbial biomass (TMB) (see Greiser and Faubel, 1988). Microbes are an important food source for meiofauna in the deep sea. The phospholipid concentration was measured colorimetrically following a chloroform-methanol extraction of the lipids from the sediment, splitting of phosphates from the lipids, and formation of a colored compound of phosphates, malachite green and ammonium-molybdate (Findlay et al., 1989; Greiser and Faubel, 1988).

In addition to microbial communities, a further significant food source for benthic organisms is the organic matter originating from primary production in the euphotic zone and reaching the deep sea as "marine snow" (Alldredge and Silver, 1988). Its amount in deep-sea sediments is estimated by determining the chloroplastic pigment equivalents (CPE), defined as the sum of chlorophyll *a* and its degradation products (i.e. phaeopigments) (Thiel, 1978). Chloroplastic pigments were extracted from the sediment with 90 % acetone by homogenization in a Precellys homogenizer. They were measured with a

Turner Fluorometer (for method see Holm-Hansen et al., 1965; Yentsch and Menzel, 1963). Hydrochloric acid (HCl) was used to differentiate between chlorophyll (CHLA) and its degraded products, phaeopigments (PHAEO). The proportion of CHLA to PHAEO (i.e. %CHLA) is used as an indicator of the 'freshness' of the organic matter (Greiser and Faubel, 1988).

The porosity of the sediment is a measure of the interstitial volume in which meiofauna can move (Giere et al., 1988). As a proxy for the sediment's porosity, water content (% H_2O) was determined by measuring the difference in weight of wet sediment samples and sediment samples dried at 70 °C.

2.4. Data processing and analyses

Statistical analyses were conducted with PRIMER7 (version 7.0.13) with the PERMANOVA + add-on and R (version 4.2.3) (R Core Team, 2023).

2.4.1. Meiofaunal communities

Meiofaunal density values were standardized to individuals per 10 cm^2 (ind. 10 cm^{-2}). Mean densities were calculated from three (pseudo-) replicates (two at station 21). Sample standard deviations were calculated to determine the among-replicate variation. Differences in meiofaunal densities among stations and sediment layers were examined with non-parametric Kruskal-Wallis-tests and post-hoc Dunn's tests; Bonferroni-corrected p-values were examined for a significance level of $p = 0.05$ (Kruskal and Wallis, 1952).

Nonmetric multidimensional scaling (nMDS) (Kruskal, 1964) was performed, based on a Bray-Curtis similarity matrix, to identify groups of samples with similar meiofaunal community composition. Due to the large differences in the density of frequent and rare taxa in the samples, meiofaunal density values were transformed ($\sqrt[4]{}$) before generating a Bray-Curtis similarity matrix. An outlier sample which contained virtually no organisms (station 22, core 1, 2–3 cm) was excluded from the analysis. A SIMPROF (similarity profile test) analysis was run to determine natural clusters in the data (i.e. SIMPROF groups, SFG). The results of the SIMPROF analysis were visualized in a nMDS plot. An ANOSIM (analysis of similarities) was performed to determine differences in meiofaunal community composition among stations.

2.4.2. Nematode biomass and nematode body form classifications

To avoid the time-consuming and rather specialized methodology of describing nematode communities by means of species composition, nematode biomass size (NBS) spectra have been developed as an alternative (Vanaverbeke et al., 2003), for which nematodes are categorized into $\log_2$ dry weight size classes. An ANOSIM was used to test for significant differences between NBS spectra, examining the sum of biomass contained in individual size classes across parallels/stations. Differences in nematode biomass among stations and sediment layers were examined with non-parametric Kruskal-Wallis tests and post-hoc Dunn's tests; Bonferroni-corrected p-values were examined for a significance level of $p = 0.05$ (Kruskal and Wallis, 1952).

The De Man ratio "A" (A = *body length/body width*) was used to classify nematodes according to their body shape (Platt and Warwick, 1988). Five body types are classified based on the De Man ratio "A" (Table 2).

Table 2
Body form classifications according to De Man ratio "A" (Platt and Warwick, 1988).

Body type	Ratio	Body form
A	0–10	Compressed
B	11–20	Plump
C	21–40	Thin
D	41–80	Slender
E	81–120	Filiform

2.4.3. Background sedimentary parameters: food proxies and porosity

For all parameters, except for bacterial abundance and biomass, mean values were calculated from (pseudo-)replicates (Table A.1). For bacterial abundance and biomass, only one sediment replicate was evaluated. Negative values were excluded.

Differences in concentrations of background sedimentary parameters between stations and sediment layers were examined with non-parametric Kruskal-Wallis tests and post-hoc Dunn's tests; Bonferroni-corrected p-values were examined for a significance level of $p = 0.05$ (Kruskal and Wallis, 1952).

A Principal Component Analysis (PCA) was conducted to explore variation in environmental characteristics between stations. However, this analysis was constrained by data availability, as samples with any missing values were excluded. To account for the reduced sample size and to better illustrate patterns of similarity among samples based on environmental characteristics, a nonmetric multidimensional scaling (nMDS) was performed. The nMDS was based on a Euclidean Distance resemblance matrix calculated from normalized values of all recorded environmental variables.

2.4.4. Correlation of meiofaunal and environmental data

A Best:BIOENV analysis was used to perform permutation tests on background sedimentary parameters (%CHLA, %H2O, bacterial abundance, organic carbon and phospholipid concentrations) to determine which parameters produce the highest correlation with meiofaunal data. Before applying the method, the environmental data was normalized and categorized with Euclidean similarities while meiofauna data were fourth root transformed and categorized using Bray–Curtis similarities. Subsequently Spearman rank correlation were calculated between these two matrices.

To further investigate the relationships between sedimentary environmental parameters and meiofaunal community composition, a distance-based linear model (DistLM) was applied. This analysis used a Bray-Curtis similarity matrix derived from meiofaunal data, with environmental predictors limited to Lipids, $\%H_2O$, chlorophyll-a (CHLA), chloroplastic pigments equivalents (CPE), and organic carbon (C-org). Due to data constraints—specifically the requirement for complete data across all replicates—bacterial abundance and biomass were excluded, as only one sedimentary replicate was available for these parameters. Both marginal and sequential tests were conducted, and the results were visualized using distance-based redundancy analysis (dbRDA).

2.4.5. Comparison of North Pole data 1996 and 2022

Differences in meiofaunal density and concentrations of environmental background parameters between 1996 and 2022 were examined with a *t*-test; p-values were examined for a significance level of $p = 0.05$.

3. Results

3.1. Meiofaunal data

3.1.1. Meiofauna composition and density

Overall, nematodes were the dominant taxon, representing ~94 % of all counted organisms, followed by Harpacticoida (~2 %), Polychaeta and Nauplii (~1 % each). Cnidaria, Kinorhyncha, Annelida, Ostracoda and Loricifera were rare, averaging 0.3 % of the total count each (Fig. 2). The highest number of taxa (6) was found at station 27 (Mendeleev Ridge), the lowest (3) at stations 22 and 21 (Makarov and Amundsen basins). At station 31, four taxa were identified.

In general, total meiofaunal densities (0–3 cm sediment depth) decreased with water depth along the sampled transect, with 335 ± 163 ind. 10 cm^{-2} at 1720 m water depth (station 31), 288 ± 124 ind. 10 cm^{-2} at 2358 m water depth (station 27), 143 ± 99 ind. 10 cm^{-2} at 3943 m water depth (station 22), and 81 ± 16 ind. 10 cm^{-2} at 4237 m

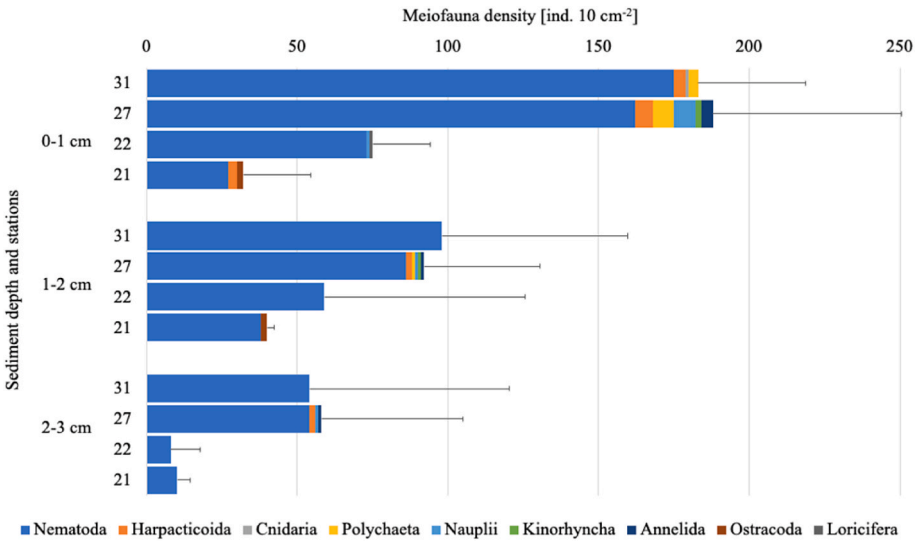

Fig. 2. Density [ind. 10 cm^{-2}] of major taxa identified at four stations (31, 27, 22, 21) and three different sediment depths (0–1 cm, 1–2 cm, 2–3 cm). Densities are shown as means of three replicates, positive error bars indicate the sample standard deviation.

water depth (station 21) (Fig. 2). Overall, looking at the sum of all sediment layers per replicate, the stations differed significantly in total meiofaunal density ($p = 0.022$). However, pairwise comparisons using Dunn's test did not identify significant differences between any specific stations after adjusting for multiple comparisons.

3.1.2. *Distribution of meiofauna over sediment depth*

At three of the four stations (22, 27, 31), a decrease of organism density with increasing sediment depth (from 0 to 3 cm) was observed (Fig. 2). At these three stations, 53–56 % of the organisms were found in the uppermost sediment layer. At station 21, however, 40 % of organisms were found in the uppermost sediment layer, and 49 % were found in the second layer. Overall, across all stations, the sediment layers differed significantly from each other ($p = 0.007$); a post-hoc Dunn's test indicated that the surface layer differed significantly from 2 to 3 cm depth ($p = 0.005$).

In addition to the decrease in the density of organisms, the taxonomic variety decreased with increasing sediment depth at three of the four stations (31, 22, and 21). In the second sediment layer (1–2 cm), two of the stations had more than one taxon present (27 and 21). In the third sediment layer (2–3 cm), only station 27 had a variety of taxa (four different major taxa), whereas at the three other sampled stations only nematodes were identified.

3.1.3. *Nonmetric multidimensional scaling of meiofaunal data*

A SIMPROF analysis identified two significant Simprof (SFG) groups (b and c), which split at a similarity of 54 % (sig. level: 1.1 %). SFG b contained principally shallow station samples (27 and 31, with station 27 represented more frequently than station 31), whereas SFG c contained mainly samples from the deeper stations (22 and 21). The SFG groups are visualized as factors in a non-metric multi-dimensional scaling (nMDS) plot (Figure B.1). An ANOSIM analysis resulted in an R-value of 0.717, indicating a high difference between the SFG groups (significance level: 0.1 %). Among-station ANOSIM indicated that the strongest differences are found between either of the deep stations (21 and 22) and station 27 (R values of 0.451 and 0.526, respectively). The difference between the deep stations and station 31 (i.e. the other shallow station besides 27) was, however, not significant.

An examination of the nMDS plot based on the meiofaunal similarity matrix with sediment depths plotted as factors indicated a rough separation of the uppermost sediment layer (0–1 cm) from the deeper sediment layers, which were loosely clustered together (Fig. 3). The

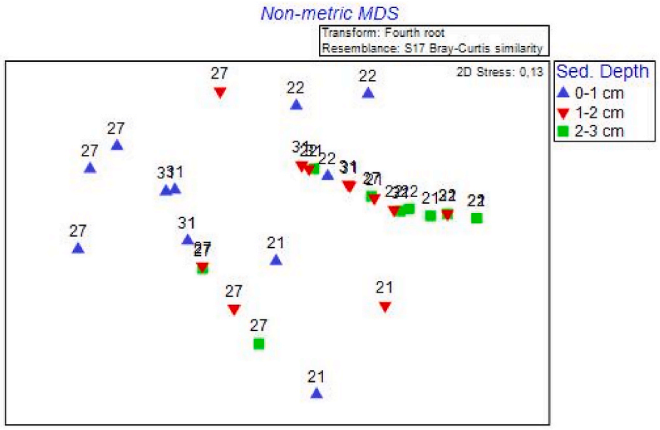

Fig. 3. Non-metric multi-dimensional scaling (nMDS) plot based on the meiofauna similarity matrix. Sediment depths (0–1 cm, 1–2 cm, 2–3 cm) are plotted as factors.

uppermost sediment layer samples were not only separated from the deeper layers, but were also spread quite far from each other, indicating a comparatively high among-station variability of the meiofauna communities found in the surface sediments. The separation between the surface and deeper sediment layers was supported by the ANOSIM results, indicating the highest difference (albeit still rather low) between the uppermost and the bottommost sediment layers ($R = 0.376$; sig. level 0.6 %). The difference between the second and third sediment layers was not significant ($R = 0.051$; sig. level 15.7 %).

3.2. *Nematode biomass and nematode body form classifications*

3.2.1. *Nematode biomass*

The difference in nematode biomass between stations overall was significant ($p = 2.2e^{-16}$); pairwise comparisons identified significant differences between all station pairs except for stations 22 and 21. In the uppermost sediment layer (0–1 cm), the biomass of nematodes decreased with increasing water depth: at station 31 (1720 m), mean nematode biomass was 7.60 ± 3.20 µg 10 cm^{-2}, and at the deepest station (station 21, 4237 m) a mean nematode biomass of 0.13 ± 0.11 µg 10 cm^{-2} was determined (Fig. 4). In the deeper sediment layers (i.e. 1-2 cm and 2–3 cm) no clear correlation between water depth and nematode

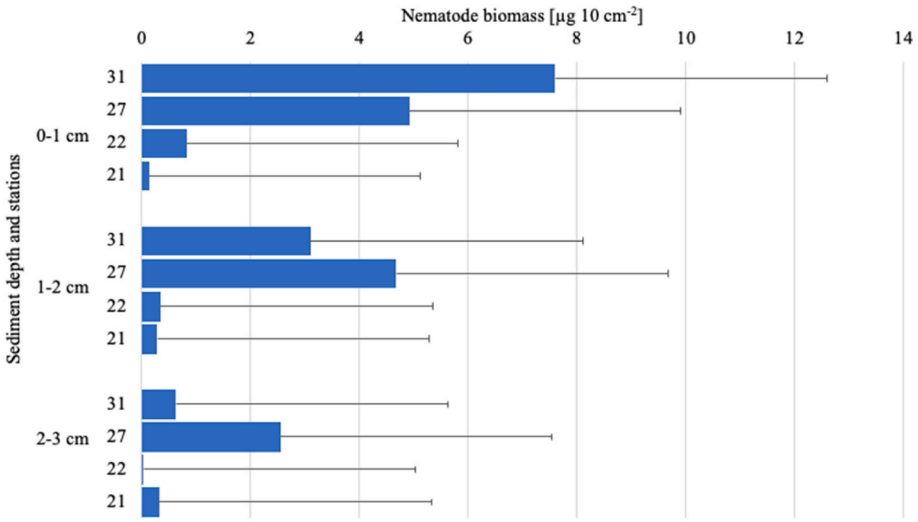

Fig. 4. Nematode biomass [mean dry weight, µg 10 cm^{-2}] at the sampling stations (31, 27, 22, 21) over sediment depths (0–1 cm, 1–2 cm, 2–3 cm). Positive error bars indicate the sample standard deviation of the replicates.

biomass was found, although the two shallower stations tend to have higher biomass than the two deeper stations. The difference in biomass across sediment layers was not statistically significant ($p = 0.3$). At station 31, a particularly large nematode (5.15 µg dry weight) was excluded from the calculations as an outlier.

The mean individual nematode biomass decreased with increasing water depth. At the shallow stations 31 and 27, the mean nematode dry weight was 0.03 ± 0.08 µg and 0.04 ± 0.10 µg, respectively. At deep stations 22 and 21, the mean dry weight decreased to 0.008 ± 0.016 µg and 0.010 ± 0.023 µg, respectively.

The trend of decreasing nematode size with increasing water depth was reflected in the nematode biomass size (NBS) spectra (Figs. 5–8, note differences in scale). At station 31, the highest biomass was located in size class 2, although it should be noted that this size class contained only one individual, the exceptionally large outlier nematode mentioned previously. Excluding this outlier, the highest biomass at station 31 is located in size class −2. With increasing water depth, the biomass peak shifted to smaller size classes: size class −2 at station 27 and size class −5 at station 22. At the deepest station, 21, the biomass peaked at size class - 3. Thus, in general, the bulk of the nematode biomass shifted to smaller size classes with increasing water depth. An ANOSIM indicated a significant difference between NBS spectra among stations ($R = 0.60$, $p = 0.009$).

In addition, the NBS spectra of the individual stations represented different size classes (i.e. the range of size classes which contain one or more nematodes). At station 31 the NBS spectrum ranged from size classes −10 to 2. At station 27, there was a slight shift towards smaller size classes, with the NBS spectrum ranging from size classes −11 to 0. At both of the deeper stations, 22 and 21, the range was shifted even further towards smaller classes, both ranging from −12 to −3.

3.2.2. *Nematode body form classifications*

At virtually all stations and sediment depths, body type “c” (thin) dominated. Body types “a” (compressed) and “b” (plump) were predominantly present in the upper sediment layers. At the deeper stations, no plump individuals were found in the deepest sediment layer. The frequency of body type “d” (slender) increased with sediment depth. Body type “e” (filiform) was rare, but it was predominately found in the deeper sediment layers (1–2 cm, 2–3 cm).

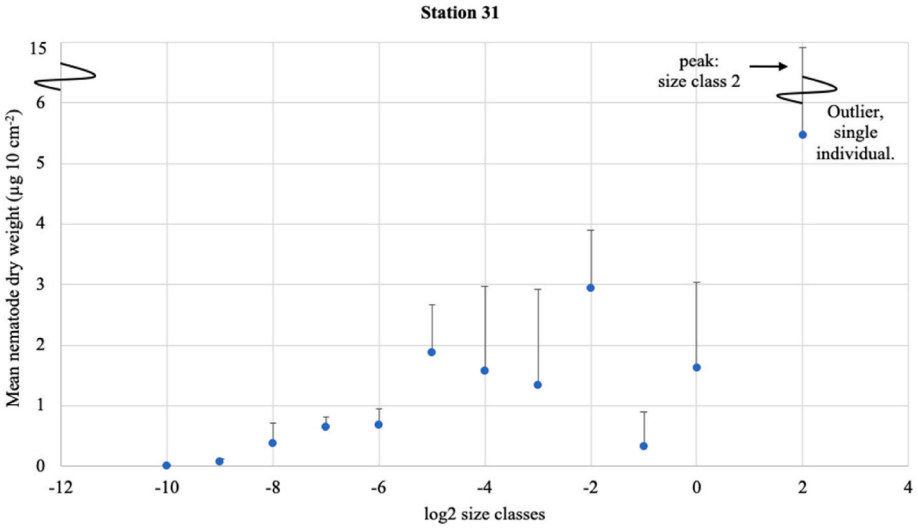

Fig. 5. Nematode Biomass Size (NBS) Spectrum at station 31 showing the mean nematode dry weight [µg 10 cm^{-2}) per log2 size class. Note break in axis scale.

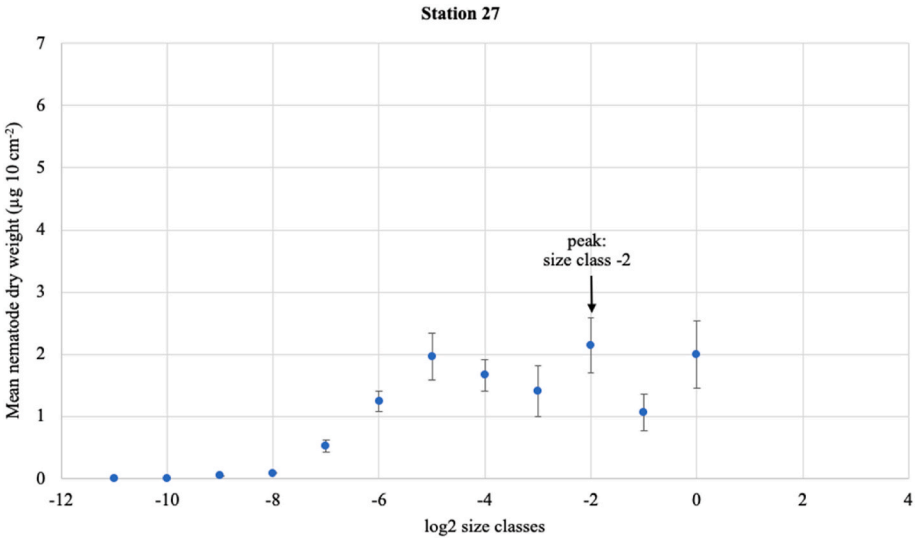

Fig. 6. Nematode Biomass Size (NBS) Spectrum plot at station 27 showing the mean nematode dry weight (µg 10 cm^{-2}) per log2 size class.

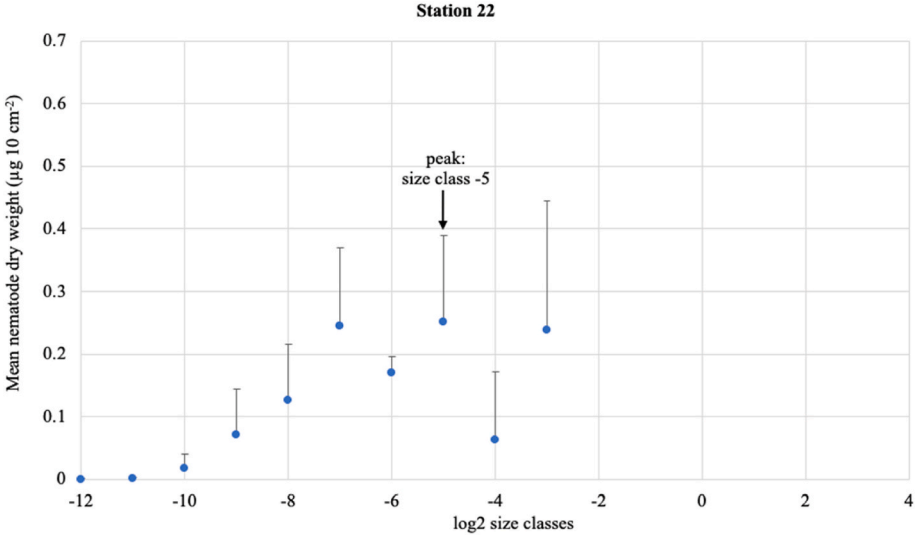

Fig. 7. Nematode Biomass Size (NBS) Spectrum plot at station 22 showing the mean nematode dry weight (µg 10 cm^{-2}) per log2 size class.

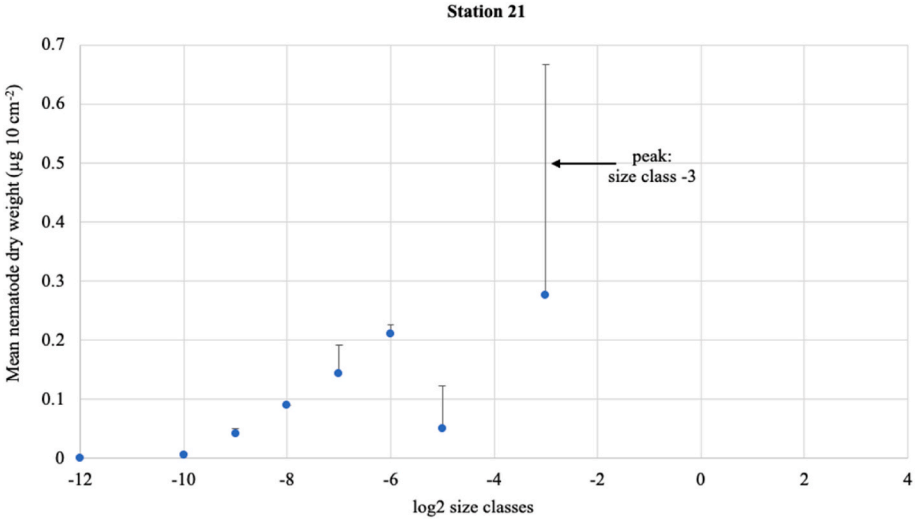

Fig. 8. Nematode Biomass Size (NBS) Spectrum plot at station 21 showing the mean nematode dry weight (µg 10 cm^{-2}) per log2 size class.

3.3. Background sedimentary parameters: food proxies and porosity

The bacterial abundance (Fig. 9) indicated lower values in the uppermost sediment layer compared to the deeper sediment layers. The overall difference between layers was significant ($p = 0.037$), but post-hoc analysis did not identify significant differences between any specific layers after adjusting for multiple comparisons. The surface layer bacterial abundance is higher in the shallow stations (2.95×10^8 cm^{-3} and 3.24×10^8 cm^{-3} at stations 31 and 27, respectively) compared to the deeper stations (1.47×10^8 cm^{-3} and 1.89×10^8 cm^{-3} at stations 22 and 21, respectively). Overall, the difference between stations was not significant ($p = 0.42$). The difference in abundance between the surface layer and the bottom layer increased from 1.76×10^8 cm^{-3} and 2.27×10^8 cm^{-3} at stations 31 and 27, respectively, to 6.23×10^8 cm^{-3} and 8.32×10^8 cm^{-3} at stations 22 and 21, respectively. A rather similar trend was seen with respect to bacterial biomass (Figure D.1).

The organic carbon content showed a clear trend at all four stations (Figure D.2): percentages were highest in the uppermost sediment layer (0.48 ± 0.04 %, 0.73 ± 0.06 %, 0.45 ± 0.01 %, 1.03 % at stations 31, 27, 22, 21 respectively) and decreased with increasing sediment depth, albeit not significantly ($p = 0.590$). Overall, there was no consistent trend in the distribution of organic carbon content with water depth (Figure D.2), although the stations differed significantly from each other ($p = 5.50\ e^{-5}$) (post-hoc Dunn's tests indicated significant differences between stations 21 and 22 ($p = 0.0002$), stations 21 and 31 ($p = 0.009$), and stations 22 and 27 ($p = 0.008$)).

Similar to organic carbon content, lipid concentrations were highest in the surface layer (4.21 ± 1.45 nmol mL^{-1}, 5.60 ± 3.26 nmol mL^{-1}, 5.78 ± 3.12 nmol mL^{-1}, 3.86 ± 1.18 nmol mL^{-1} at stations 31, 27, 22, 21 respectively) and decreased with increasing sediment depth (in deepest sediment layer: 3.70 ± 1.01 nmol/mL, 1.63 ± 0.44 nmol mL^{-1}, 2.90 ± 1.88 nmol mL^{-1}, 2.54 ± 1.21 nmol mL^{-1} at stations 31, 27, 22, 21 respectively) (Figure D.3). Lipid concentrations were slightly higher at the mid-depth stations (27, 22) (Figure D.3), but overall there was no significant trend with water depth ($p = 0.51$).

At the shallow stations, the highest %CHLA was found in the surface sediments (9.38 ± 2.55 % and 18.91 ± 5.51 % at stations 31 and 27 respectively), and the proportion decreased with increasing sediment depth (4.44 ± 0.03 % and 4.35 ± 1.74 % in deepest layer at stations 31 and 27 respectively) (Fig. 10). At the deeper stations, the highest proportion of chlorophyll *a* was found in the second sediment layer (10.03 ± 2.33 % and 7.61 ± 4.52 % in the second layer compared to 4.76 ± 1.26 % and 3.88 ± 3.40 % in the surface layer and stations 22 and 21 respectively). Differences between sediment layers were not statistically significant ($p = 0.25$), nor were the differences between stations ($p = 0.67$).

Overall, CPE concentrations decreased with increasing sediment depth (Figure D.4), albeit the differences were not significant ($p = 0.075$). Overall, there was no consistent trend in the distribution of CPE with water depth, although the stations differed significantly from each other ($p = 7.55\ e^{-5}$) (post-hoc Dunn's tests indicated significant differences between stations 22 and 21 ($p = 7.84\ e^{-5}$), stations 22 and 27 ($p = 0.0053$)).

The phaeophytin (PHAEO) concentrations decreased with increasing sediment depth at all four stations (Figure D.4); the difference between layers was significant ($p = 0.042$). Pairwise comparisons of the post-hoc Dunn's tests indicated significant differences between the surface layer and 2–3 cm depth ($p = 0.0406$). Differences between stations overall were significant ($p = 6.37\ e^{-5}$). Post-hoc analysis identified significant differences between stations 22 and 21 ($p = 0.00007$), as well as between stations 22 and 27 ($p = 0.003$).

The water content (%H2O) decreased with increasing sediment depth at all four stations (Fig. 11) but these differences were not statistically significant ($p = 0.052$). Along the transect, there was a slight decrease from station 31 to station 27 (63 % and 47 % in the surface layer, respectively), followed by an increase at the deeper stations (56 % and 67 % in the sediment surface layers at stations 22 and 21, respectively). The highest water content was found at the deepest station. Differences among stations were significant ($p = 0.007$). Post-hoc analysis identified station 22 as significantly different from station 27 ($p = 0.009$).

A Principal Component Analysis (PCA; Figure C.2) revealed no distinct separation among stations, except for the uppermost sediment layer at station 27, which appeared clearly distinct from all other samples. In the nMDS plot, the samples taken in the uppermost sediment layer are separated from those taken in the 2–3 cm sediment layer (Fig. 12). Differences in environmental parameters are more prominent among sediment depths than among stations (i.e. water depths). ANOSIM indicated that this difference in the environmental setting was significant (0–1 cm vs. 2–3 cm: $R = 0.303$, sig. level 0.1 %). There was no significant difference between the second and third sediment layer (1–2 cm vs. 2–3 cm: $R = 0.063$, sig. level 11.6 %).

3.4. Meiofauna and environmental data

As identified by a Best:BIOENV analysis, the most important variable structuring meiofaunal communities was %CHLA (BEST correlation: 0.231). The most important groups of variables encompassed %H2O and

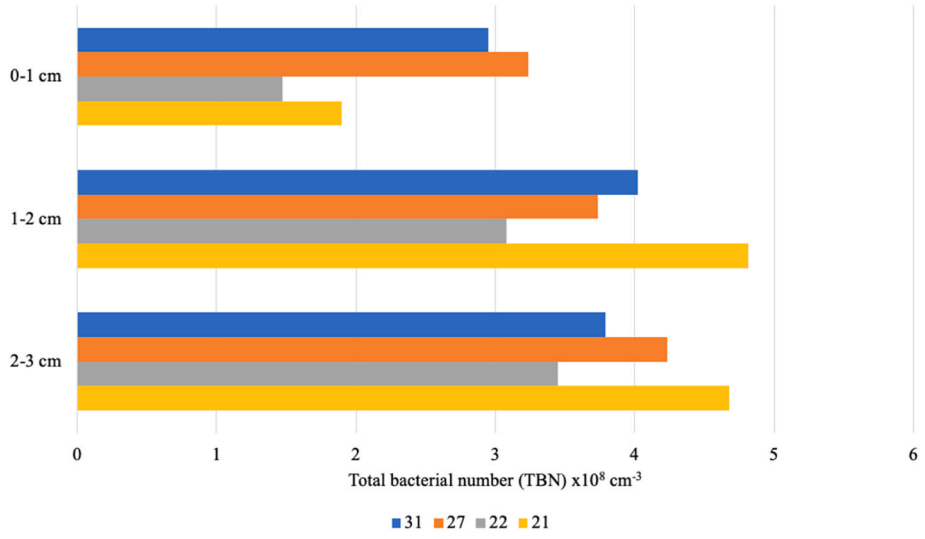

Fig. 9. Bacterial abundance [total bacterial number (TBN) x10^8 cm^{-3}] at the sampling stations (31, 27, 22, 21) over sediment depths (0–1 cm, 1–2 cm, 2–3 cm).

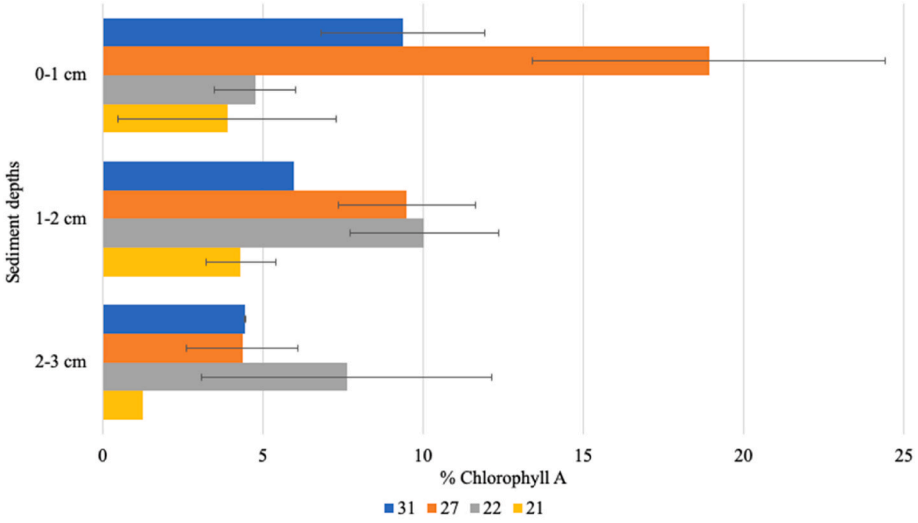

Fig. 10. Percentage chlorophyll *a* (%CHLA) at the sampling stations (31, 27, 22, 21) over sediment depth (0–1 cm, 1–2 cm, 2–3 cm). Error bars indicate the sample standard deviation.

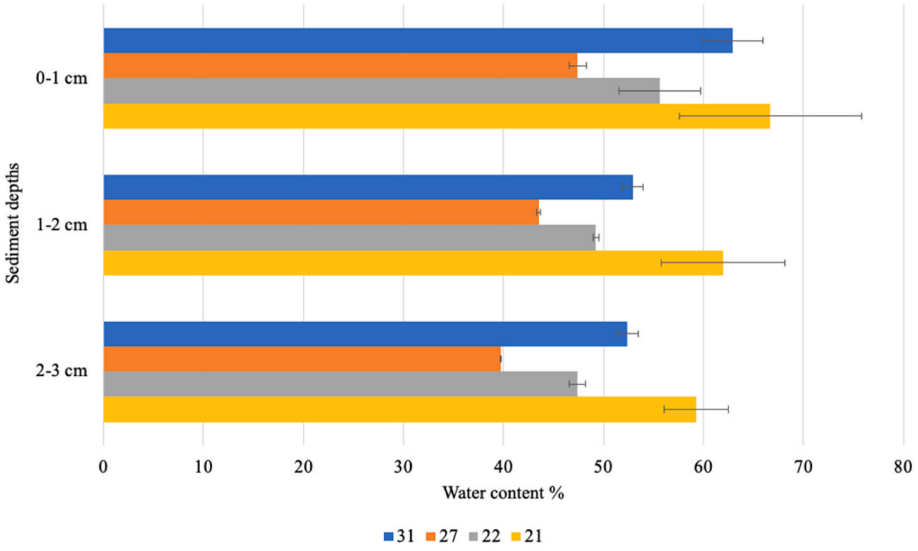

Fig. 11. Water content (%H2O) at the sampling stations (31, 27, 22, 21) over sediment depth (0–1 cm, 1–2 cm, 2–3 cm). Error bars indicate the sample standard deviation.

%CHLA (correlation: 0.401), and %H2O, %CHLA and bacterial abundance (correlation: 0.400). The addition of further parameters (i.e. LIPID and C-org) did not increase the BEST correlation.

The full DistLM was visualized by examining the dbRDA ordination (Fig. 13). The first two dbRDA axes captured nearly 94 % of the variability in the fitted model, accounting for approximately 42 % of the total variation in the meiofaunal community data. The vector overlay indicated that the first dbRDA axis was primarily associated to %H2O and organic carbon content, while variables indicative of food availability (CPE, CHLA, LIPIDS) were more closely aligned with the second dbRDA axis. Among the predictive variables, %H2O showed the strongest association with dbRDA1, whereas food availability in terms of CHLA had the strongest association with dbRDA2.

The DistLM analysis identified sediment water content (%H_2O) and chlorophyll *a* concentrations (CHLA) as the most influential environmental predictors of meiofaunal community composition. Each variable individually explained over 20 % of the observed variation (%H_2O: $p = 0.0085$; CHLA: $p = 0.0064$). Although organic carbon content (C-org %) was not significant in the marginal test ($p = 0.58$), it became significant in the sequential test ($p = 0.0496$), contributing an additional 11.3 % to the explained variation. In contrast, lipid content and chlorophyll-derived pigments (CPE) had negligible influence on community structure (both $p > 0.47$), each explaining less than 4 % of the variation. Altogether, the environmental variables included in the DistLM model accounted for approximately 45 % of the total variation in meiofaunal assemblages.

3.5. *Meiofaunal communities and food proxies at the North Pole in 1996 and 2022*

3.5.1. *Meiofaunal data*

The meiofauna samples taken at the North Pole in 1996 (Schewe and Soltwedel, 1999) and 2022 (this study) were both characterized by little diversity and low overall densities (Table 3). Nematoda was the dominant taxon in both years. Both sampling campaigns identified only two non-nematode groups (Harpacticoida and Ostracoda in 2022 and Harpacticoida and Nauplii in 1996"). Sediment layers sampled in 1996 and 2022 did not differ significantly from each other ($p = 0.78, 0.15, 0.90$ for

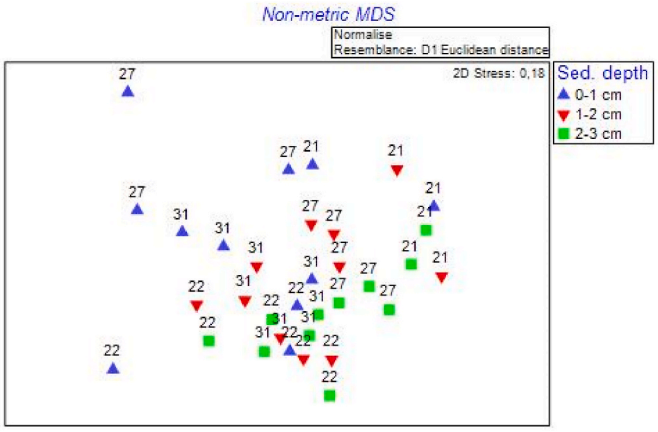

Fig. 12. Non-metric multi-dimensional scaling (nMDS) plot based on the environmental data resemblance matrix. Sediment depths (0–1 cm, 1–2 cm, 2–3 cm) are plotted as factors.

sediment depths 0–1 cm, 1–2 cm, and 2–3 cm respectively).

3.5.2. Food proxies

In the surface sediments (0–1 cm), measured lipid concentrations were rather similar between 2022 and 1996 (3.86 ± 1.18 nmol/mL and 3.70 ± 1.32 nmol/mL, respectively) (Figure E.1). In the deeper sediment layers, lipid concentrations were higher in 1996 than in 2022 (1–2 cm: 5.04 ± 0.18 nmol/mL (Schewe and Soltwedel, 1999) vs. 2.81 ± 1.90 nmol/mL (this study)). The sampled sediment depths did not differ significantly from each other (p = 0.90, 0.34, 0.56 for sediment depths 0–1 cm, 1–2 cm, and 2–3 cm respectively).

In the surface sediments (0–1 cm), bacterial abundance was slightly higher in 1996 than in 2022 (3.61×10^8 cm^{-3} vs. 1.89×10^8 cm^{-3}) (Figure E.2). In the deeper sediment layers, abundances were lower in 1996 than in 2022 (3.21×10^8 cm^{-3} vs. 4.68×10^8 cm^{-3}).

For both chlorophyll and phaeophytin concentrations (i.e. CPE) at all three sediment depth layers, higher concentrations were measured in 2022 then in 1996 (Fig. 13). The difference between sampling years across all layers was significant (p = 0.007). In the surface layer, a CPE concentration of 0.24 ± 0.01 μg mL^{-1} was measured in 1996 while in 2022 it was 3.50 ± 0.75 μg mL^{-1}.

Although notably higher absolute concentrations were measured in 2022, the proportions of "fresh" material, i.e. %CHLA, were significantly higher (p = 0.005) in 1996 (Fig. 14). During "Arctic Ocean '96" there was little variation in %CHLA over sediment depth (8.46 ± 1.45 %, 7.81 ± 1.68 % and 8.06 ± 3.68 % from 0-1 cm to 2–3 cm sediment layer), whereas in HLY2202 samples a clear decrease is noted in the 2–3 cm sediment layer (3.88 ± 3.40 % in 0–1 cm layer, 1.24 % in 2–3 cm layer) (see Fig. 15).

4. Discussion

4.1. Food in the deep sea: a scarce good

Food and oxygen are the "two most important conditions indispensable to benthos life" (Thiel, 1983). Both originate virtually exclusively from the surface production and the water column above the seabed, with the exception of certain specialized deep-sea habitats (e.g. hydrothermal vents, cold seeps) (Ingels et al., 2023b; Vanreusel et al., 2023). Within the water column, microbial activity and macro- and microplankton consume and rework much of the sinking material (i.e. particulate organic matter, POM) (Azam and Malfatti, 2007; Grebmeier and Barry, 1991; Suess, 1980). In the deep sea, due to the long residence time of POM within the water column, food reaches the benthic environments in low quality and quantity, resulting in general food limitation (Grebmeier and Barry, 1991). In the Arctic, this pattern is particularly pronounced due to the limited primary productivity in the permanently ice-covered regions, resulting in a strong coupling between the seasonal surface production and the benthic communities along the ice margins (Ingels et al., 2023a). In the present study, the one station (31) that was not permanently ice-covered in 2022 did not differ from

Table 3
Densities of meiofauna (ind. 10 cm^{-2} across 0–3 cm sediment depth) collected at the North Pole during the "Arctic Ocean '96" expedition of 1996 and HLY2202 in 2022.

	"Arctic Ocean '96"	HLY2202
Nematoda	55 ± 7	75 ± 20
Harpacticoida	1 ± 2	3 ± 0
Nauplii	2 ± 2	0
Ostracoda	0	3 ± 5
Unidentifiable meiofauna	2 ± 2	0

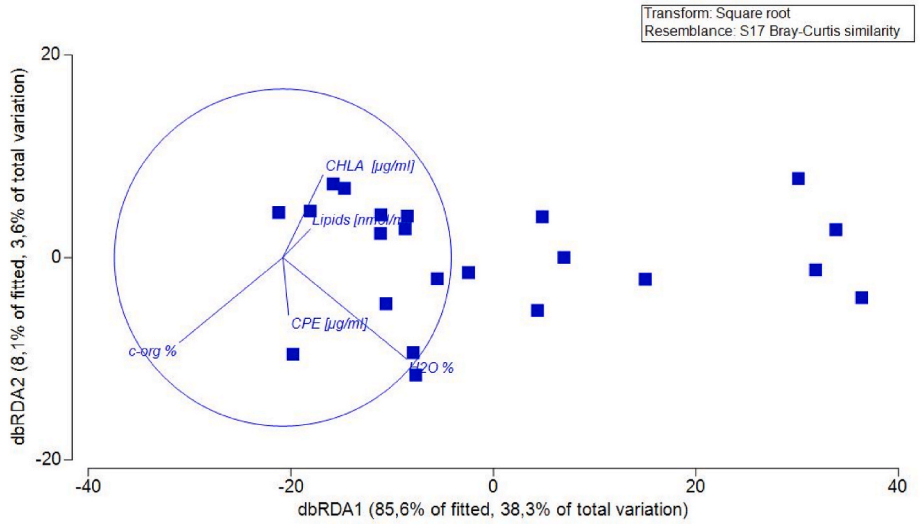

Fig. 13. Distance-based redundancy analysis (dbRDA) ordination investigating the relationship between meiofaunal communities and sedimentary environmental parameters; CHLA = chlorophyll *a*, Lipids: phospholipids, CPE: chloroplastic pigment equivalents, %H2O: water content, c-org% = organic carbon. The length of the overlying vectors indicates the strength of correlation with the axes.

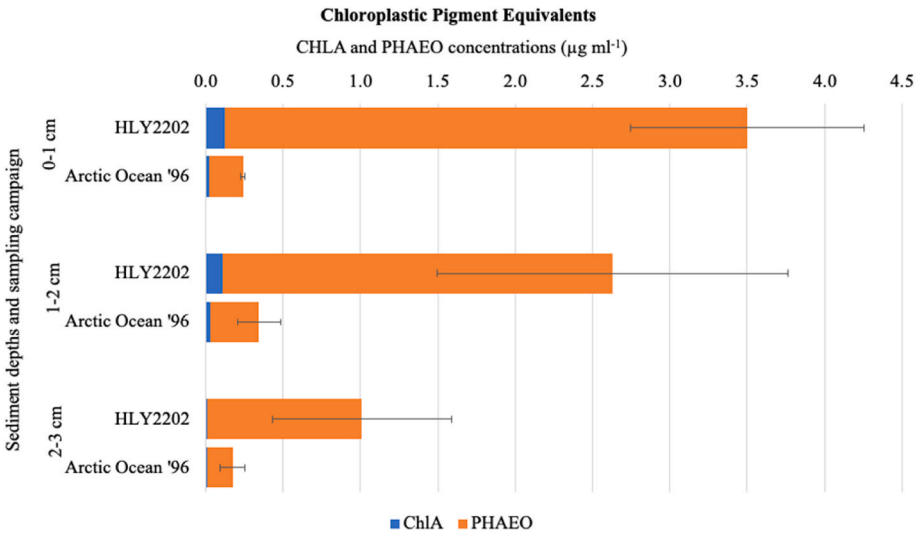

Fig. 14. CHLA and PHAEO concentrations [µg mL^{-1}] over sediment depth (0–1 cm, 1–2 cm, 2–3 cm) sampled at the North Pole in 1996 (Arctic Ocean '96) and 2022 (HLY2202). Error bars indicate the sample standard deviation.

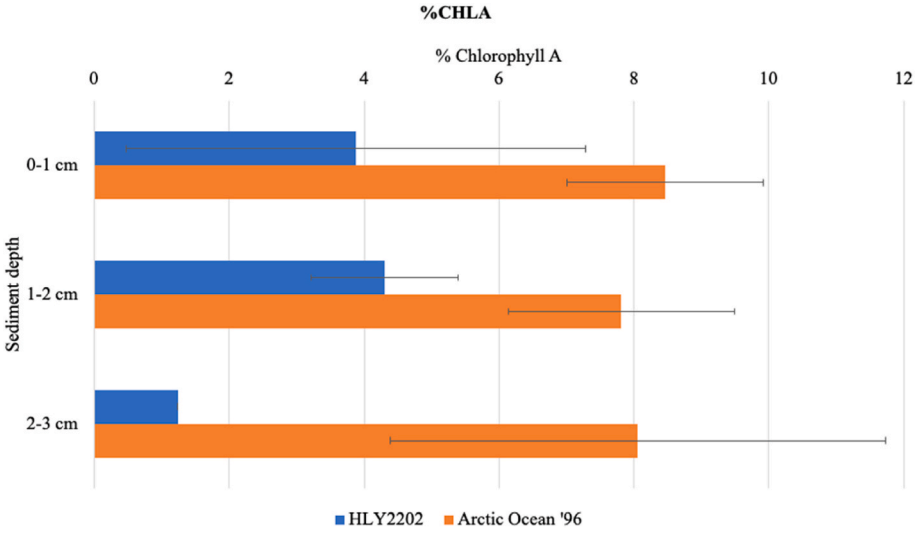

Fig. 15. Percentage chlorophyll *a* (%CHLA) over sediment depth (0–1 cm, 1–2 cm, 2–3 cm) sampled at the North Pole in 1996 (Arctic Ocean '96) and 2022 (HLY2202).

the other stations along the transect with regard to food proxies indicating organic matter input from primary production. However, no general conclusion about the impact of sea ice coverage on vertical fluxes and food availability at the seafloor can be drawn from this single sampling event, particularly given uncertainties such as timing and location of the phytoplankton bloom.

As described by Soltwedel and Schewe (1998): "the deep Arctic Ocean is probably one of the most oligotrophic marine ecosystems on Earth", and the results of the present study confirm this notion. Of the food proxies evaluated (i.e. organic carbon, phospholipids, bacterial abundance and biomass, phaeophytins and the proportion of chlorophyll), three show trends with water depth. Bacterial abundance and biomass both show decreasing surface values with increasing water depth. No trend is seen in the deeper sediment layers, however. Although absolute concentrations of phaeophytin and CPE showed no water-depth correlation (the lowest phaeophytin concentration was found at station 22, the highest at station 21, i.e. the two deep stations), the relative proportion of fresh material (%CHLA) in the surface layer indicated a decreasing trend with increasing water depth. The other parameters indicating food availability, organic carbon and lipid concentration, showed no correlation with water depth. It is noteworthy that in the Central Arctic bathymetric gradients are not isolated but often coincide with both latitudinal gradients and distance from the continental shelf. As such, the role of depth in shaping food availability may be confounded with, or even outweighed by latitudinal effects on primary productivity (Renaud et al., 2006) and the proximity of sampling stations to the base of shelf slopes, where enhanced food input and benthic activities have been observed (Clough et al., 2005; Kiesel et al., 2020).

A comparison of the results of the present study with a previous study (Soltwedel and Schewe, 1997) in the same region (central Arctic) shows similar trends. Soltwedel and Schewe (1998) similarly found a highly significant relationship between bacterial abundance/biomass and water depth. In contrast, they found a decrease over sediment depth, whereas the present study found an increase. With regard to sediment phospholipid concentrations, Soltwedel and Schewe (1998) also discovered the lack of a direct correlation with water depth but a decreasing trend with increasing sediment depth. As sediment

phospholipid concentrations indicate the total microbial biomass, which includes not only bacteria but also *inter alia* fungi, protozoa and micrometazoa, the difference in trends between TBN and phospholipid concentrations may be caused by a high proportion of this "other" microbial biomass in the deep sea (Soltwedel and Schewe, 1997). For CPE and %CHLA, Soltwedel and Schewe (1998) observed the same trend as in the present study: %CHLA was higher at shallower stations, and no significant trend was found for CPE across water depths. Soltwedel and Schewe (1998) argue that this indicates some decoupling of the central Arctic deep sea from the primary production at the ice edge and continental margin, although lateral transport and ice-algae production still result in benthic-pelagic coupling in ice-covered regions (Zhulay et al., 2023).

Overall there is some evidence of a food-limited deep-sea environment along the sampled transect, although not all sedimentary food proxies examined support this trend.

4.2. Patterns in meiofaunal community properties

4.2.1. Meiofaunal community composition and distribution

Nematodes are typically the most abundant metazoan meiofaunal group in deep-sea sediments, often representing over 90 % of the sedimentary metazoans, followed by Harpacticoida/Copepoda, Nauplii and Polychaeta (Giere and Schratzberger, 2023; Rosli et al., 2018). This corresponds to the dominant taxa identified in the present study, indicating that the meiofaunal community composition along the sampled transect is consistent with community composition described for other deep-sea regions (Rosli et al., 2018).

Within the sediment, the number of identified taxa, as well as meiofaunal density, is highest in the surface layer and decreases with increasing sediment depth. The difference between the sediment surface and deeper layers is also visible in the nMDS plot showing the pattern of among-sample differences in meiofaunal community composition. This pattern has been well documented throughout earlier studies (e.g. Schewe, 2001; Schewe and Soltwedel, 1999; Schnier et al., 2023; Soetaert et al., 2002; Soltwedel and Schewe, 1998), and can largely be explained by the fact that the surface layer receives higher input of particulate organic matter (POM) from the water column above. The surface sediment is therefore also most susceptible to the patchiness caused by pulsed POM influx. Evidence of this was seen in the pronounced spread of surface layer samples in the nMDS plots of both environmental sedimentary parameters and the meiofaunal samples.

In the present study, meiofaunal densities decreased with increasing water depth, as is generally the case in many observations (Grzelak et al., 2017; Schewe, 2001; Schewe and Soltwedel, 1999; Schnier et al., 2023; Soltwedel and Schewe, 1997). This water depth-related trend is also visible in meiofaunal community composition. Such gradients in faunal composition and density are most often associated with differences in organic matter input (see above).

The number of major taxa identified at each station along the transect was higher at shallow stations than at deep stations. Diversity gradients in relation to water depth have been subject of many studies, with varying trends being found (Grzelak et al., 2017; Schnier et al., 2023; see Vanreusel et al., 2023 for full discussion). However, the present study is limited by the identification of taxa at gross taxonomical resolution. More detailed taxonomic identification to genus or species level is required to contribute meaningfully to the study of diversity patterns along the transect.

4.2.2. Nematode biomass and miniaturization

The total nematode biomass per station decreased with increasing water depth – a trend that has been well documented in several studies (see e.g. Soetaert et al., 2002). This pattern can, in part, be explained by the decrease in nematode abundance at deeper stations. However, a further factor is the decrease in nematode size with increasing water depth, both in mean individual biomass and the shift towards smaller size classes.

Miniaturization is a well-documented adaptive trait among deep-sea organisms, particularly meiofauna, and is often seen as a response to the extreme oligotrophic conditions at depth. Smaller body size offers benefits, such as lower metabolic demands, a higher surface-area-to-volume ratio for nutrient uptake, and shorter generation times that may enhance reproductive success in variable environments (Giere, 2009; Thiel, 1975). However, these advantages come with trade-offs, including limited dispersal, lower energy reserves, and increased susceptibility to predation (Levin and Gage, 1998; Soetaert and Heip, 1995).

Although many studies observe a decrease in body size with increasing water depth (e.g. Ansari et al., 2017; Soltwedel et al., 1996; Udalov et al., 2005), they stress the need to distinguish between "water depth" and "limited food availability" as drivers of this trend. Hydrostatic pressure is not considered a primary factor, and in the Central Arctic, overlapping gradients like latitude and shelf proximity may influence food availability and productivity (Udalov et al., 2005).

Miniaturization in nematodes, reflecting r-strategist traits, is common in more unpredictable environments, such as deeper stations where food is patchy (Hasemann, 2006; Schewe and Soltwedel, 1999). Despite challenges in using mean body mass as a metric due to outliers (Kaariainen and Bett, 2006), a clear trend toward miniaturization with depth was observed, suggesting that food availability—particularly sediment organic matter—plays a central role in driving this pattern (see Chapter 4.1).

4.3. Drivers of meiofaunal community composition

4.3.1. Impact of food proxies

In this study, two parameters related to food input were recognized as main drivers of meiofaunal community patterns: %CHLA and bacterial abundance. However, other parameters, like organic carbon and phospholipid content, showed no significant correlation with meiofaunal densities.

Studies generally agree on the importance of CPE and bacterial abundance (or biomass) as the main drivers of the distribution of meiofauna (e.g. Schewe, 2001), even though this relationship was not always visible in the data (e.g. Schewe and Soltwedel, 1999). Grzelak et al. (2017) state that fresh organic matter is preferred by nematodes over bacteria as food source, whereas Ingels et al. (2010) describe an experimental result indicating that bacteria are preferred over fresh phytodetritus. The lower bacterial abundance and biomass in the upper sediment layer compared to deeper sediment layers in the present study could potentially indicate the effect of consumption by meiofauna. The present study indicates a slightly higher correlation between meiofauna and comparatively fresh phytodetrital matter (i.e. %CHLA) than between meiofauna and bacterial abundance, but both may be considered an important source of food for meiofaunal organisms.

Phosopholipid concentrations were not correlated with meiofaunal densities. Organic carbon concentrations were found to be significant in a sequential DistLM analysis, indicating that the impact of organic carbon is context-dependent, modulated by physical, chemical, and biological interactions in sediments. This could potentially suggest the use of c-org as a synergistic indicator of environmental condition and energy availability over longer timescales (Aller, 1994; Middelburg, 2018; Smith and Demopoulos, 2004; Snelgrove and Butman, 1994). Schewe and Soltwedel (1999) suggest the complex trophic interrelations between meiofauna and the wide variety of microorganisms, which contribute to the phospholipid parameter, as a reason for the lack of a clear correlation. Along the bathymetric HAUSGARTEN transect, chlorophyll *a*, bacterial abundance and %H2O were more important drivers of community composition in the upper and lower bathyal zone, whereas phospholipids were more important at greater water depths in the abyssal zone (Schnier et al., 2023), linking to potential impacts of distance to shelf (Kiesel et al., 2020). To detect such a pattern along the

transect examined in the present study, more stations need to be examined (Table A.2).

4.3.2. Impact of sediment water content

The second most important factor driving meiofaunal community patterns in this study is a physical sediment parameter, the sediment water content. It indicates the mass of water in relation to the wet mass of a sediment sample and can be used as a rough parameter of the sediment porosity (Giere, 2009). Sediment porosity, the total pore volume of a sediment sample, depends on the shape, sorting and mixing of sediment particles (Giere, 2009). Both porosity and water content are related to sediment grain size, which is "fundamental to all ecological aspects of meiobenthic work" (Giere, 2009; Vanreusel et al., 2023).

Interstitial space of a sediment (i.e. porosity) is of key importance to meiobenthic organisms. For example, it influences spatial and structural habitat conditions and the circulation of pore water (Giere, 2009; Wieser, 1959). Correlations between sediment characteristics, including grain size and water content, and meiofaunal organisms, particularly in terms of mobility, are well documented (Giere and Schratzberger, 2023; Schratzberger and Larcombe, 2014).

Wieser (1959) classified small invertebrates in sediments according to their mobility either as "burrowers" (i.e. pushing through the sediment medium) or "sliders" (i.e. moving through the interstitial spaces). Classification of nematodes into either "burrowers" or "sliders" using the De Man (length/width) ratio "A" distinguished two nematode morphotypes (Soetaert et al., 2002): long and slender (high L/W ratio) opposed to short and stout (low L/W ratio). The long and slender nematodes prefer deeper sediment layers due to their increased mobility, whereas the short and stout individuals "pay for obesity with reduced mobility", which is why they are constricted to the uppermost sediment layers with relatively high porosity (Soetaert et al., 2002).

Thus, according to Soetaert et al. (2002), the detected trend in the present study of stout/shorter nematodes in the upper sediment layers and the percentage increase of longer/slender nematodes in the deeper sediment layers could be explained by the reduced mobility of De Man ratio "A" classes A (compressed) and B (plump), causing their concentration in the upper layers with highest water content (i.e. porosity). The slender nematodes, which are, up to a certain sediment density (i.e. pore volume), not limited by their size, can move throughout the sediment column, and can therefore exist in deeper, denser sediment.

However, it is also important to note that an earlier study by Tita et al. (1999) found a contrasting correlation: in muddy sediments (with little interstitial space) nematodes were thicker than in sandy sediments (i.e. with relative large interstitial space). The authors argue that the wider nematodes can burrow and actively relocate sediment particles, and can therefore move through denser sediments, while slender nematodes must be thin enough to move through the interstitial space, and are therefore more abundant in more porous sediments (Tita et al., 1999).

4.3.3. Unidentified drivers

In this study, a combination of food proxies and sediment water content contributed most to the explanation of the variability in meiofaunal communities along the sampled transect. However, these parameters together only accounted for a relatively low correlation (% CHLA, %H2O, bacterial abundance, correlation: 0.400), clearly indicating that the meiofaunal community patterns are also influenced by further parameters that are not considered in this study.

Vanreusel et al. (2023) reviewed the knowledge about environmental drivers of meiofaunal diversity patterns. Although these factors include substrate type (such as sediment granulometry and %H2O) and organic matter supply (i.e. food parameters), many other drivers are also important, both abiotic factors, like oxygen, temperature, disturbance, salinity and, even more importantly, biotic factors such as interactions with other ecosystem components. These interactions can encompass, for example, predation and intra- and interspecific competition, as well as bioturbation.

Another aspect that influences the distribution of nematodes within the sediment (but has not been considered in this study) is the oxygenation of the pore water, which is related to the sediment water content (Soetaert et al., 2002). Slender nematodes may be better adapted to hypoxic conditions, allowing them to survive in deeper sediment layers with reduced oxygen concentrations. The slender, elongated bodies of these nematodes provide a higher surface area relative to their volume. This is advantageous in hypoxic environments because it allows for more efficient gas exchange across their body surface, which is critical when oxygen availability is limited. This adaptation allows them to absorb the small amounts of dissolved oxygen present in deeper, oxygen-deprived sediments. Slender nematodes may also move deeper into sediment layers to escape predators or competition; thicker nematodes, due to their bulky body form (especially members of the Desmoscolecidae family with thick desmen), are more protected from predation in the surface sediments than slender individuals.

The potential importance of such unidentified drivers, which were not considered in this study, is particularly pronounced for station 27. It stood out in the PCA, had the highest number of major taxa, was most variable among all three examined sediment horizons, and was significantly different from the deep stations (22 and 21), unlike the other shallow station (31). Moreover, it distinctly dominates SFG b, suggesting a clear separation from the other stations analyzed. This pattern highlights the influence of factors unrelated to water depth, which were not explored in this study. Expanding the analysis to include additional stations in this vicinity (Table A.2) would provide valuable insights into this pattern.

4.4. Meiofauna and food proxies at the North Pole in 1996 and 2022

There was virtually no difference in the composition of meiofaunal communities sampled at the North Pole in 1996 and 2022 at a gross taxonomic level (Table 3). Moreover, sediment food proxies differed only with regard to chlorophyll and phaeophytin: the absolute concentrations of both parameters were higher in 2022, while the proportions of fresh material (i.e. %CHLA) were higher in 1996. Although the sampling events at the North Pole were conducted within the same seasonal period, a notable increase in degraded sediment pigments was observed in 2022 compared to 1996. This difference may be attributed to several factors, such as variations in the timing of the phytoplankton bloom, differences in bloom composition with regard to degradability, or changes in current patterns that influenced the deposition of material. As Ambrose and Renaud (1997) showed, large pulses of phytopigments can disappear within a month (Clough et al., 2005). These insights suggest that while direct conclusions about long-term ecosystem changes cannot be drawn from just these two events, they provide valuable context for further investigation.

In general, there is overwhelming evidence that the Arctic is changing at an extraordinarily rapid pace, and Arctic amplification is also well documented (Graversen et al., 2008; Piepenburg, 2005; Previdi et al., 2021). Grebmeier et al. (2006) outlined a major ecosystem shift in the shallow northern Bering Sea shelf, confirming expected climate effects in the Pacific-influenced Arctic. The common notion that the deep sea is "buffered" and less affected by climate change has been contradicted by several studies (Lampitt, 1985; Paulus, 2021). Rogers (2015) concludes his review by stating that "deep-sea ecosystems are likely to be highly sensitive to changes in food supply and the physical environment driven by global climate change".

Therefore, the finding of this study that meiofaunal communities at the North Pole station did not change in the 26 years between 1996 and 2022 is surprising. However, it is important to note that the present study was confined to analyses at gross taxonomic resolution. Consequently, any changes in diversity at species or genus level, as they have been documented in response to climate change in other regions (e.g.

Grebmeier et al., 2006), could not be detected. Moreover, while the primary production in the Arctic Ocean is generally affected by the changing global climate, due to reduced sea-ice coverage, increasing water-column stratification, altered nutrient availability, and increased microbial metabolism due to higher temperatures (Frey et al., 2020; Gaffey et al., 2022; Rogers, 2015), these processes are particularly strong in the marginal ice zones and along continental Arctic shelves. While the still permanently ice-covered North Pole region is also affected by thinning multi-year ice and related changes in ice-algae production, the resulting changes in benthic-pelagic coupling and, subsequently, meiobenthic community patterns are currently very likely still less pronounced than in the more southern marginal ice-zone regions.

5. Summary and perspectives

This study of meiofaunal communities along a bathymetric and latitudinal transect in the western Arctic Ocean confirmed a number of notions based on consistent findings from previous studies: meiofaunal density and the variation of taxa decreased with both increasing water depth and sediment depth, and nematodes decreased in body size with increasing water depth. As observed in previous research, these trends were closely linked to indicators of food availability. Consistent with earlier findings, chlorophyll *a* and bacterial abundance emerged as key food sources supporting meiofaunal communities. Sediment porosity was also found to correlate with meiofaunal densities, and it is also an important factor driving the variation of nematode body shapes with sediment depth: thicker nematodes were predominantly found in the surface sediments, while slimmer individuals were present in deeper sediment layers, suggesting differences in mobility in relation to interstitial space.

Virtually no differences were found in the abundance of meiofaunal taxa at the North Pole recorded in 1996 and in 2022. This may be related to relative stability of the still ice-covered central Arctic compared more intense changes in the marginal ice zones. Some differences were noted in the quality and quantity of phytopigments between the sampling years, potentially related to the timing of sampling in relation to the bloom.

Further investigations necessary to strengthen and extend the findings of this study include: (1) Examining the meiofaunal composition at genus level, with a focus on the dominating taxa (i.e. nematodes) to allow for addressing potential changes in diversity and ecosystem functions in relation to environmental changes (Vanreusel et al., 2023). (2) Examining further stations of the HLY2202 transect to increase the spatial resolution of the results and conclusions about conditions and trends documented in this study (see Table A.2 for all sampled stations visited during the HLY2202 cruise). (3) Combining the results of the present study on the meiobenthos with those from other concomitant investigations during the HLY2202 cruise, such as analyses of macrobenthos communities, as well as water-column chlorophyll, phaeophytin and POM data (Ashjian and Grebmeier, 2024).

CRediT authorship contribution statement

Jona R. Silberberg: Writing – review & editing, Writing – original draft, Methodology, Investigation, Formal analysis. **Dieter Piepenburg:** Writing – review & editing, Supervision, Conceptualization. **Christiane Hasemann:** Writing – review & editing, Supervision, Methodology, Conceptualization.

Data availability

The HLY2202 data generated for the present study can be accessed here: https://data.mendeley.com/preview/6t5ks9rm4j?a=d44ff3c6-8ea3-46c6.

The reference data used for the time comparison at the North Pole can be accessed here: doi.pangaea.org/10.1594/PANGAEA.738504

Funding sources

Sampling for this study was supported by the National Science Foundation [grant number 2053101]; and the International Arctic Science Committee (Marine Working Group) [Enabling Early Career Scientist and/or Indigenous Participation in Internationally Cross-Platformed Research Cruises].

Declaration of competing interest

The authors declare the following financial interests/personal relationships which may be considered as potential competing interests: Jona Rebekka Silberberg reports financial support was provided by National Science Foundation. Jona Rebekka Silberberg reports financial support was provided by International Arctic Science Committee. If there are other authors, they declare that they have no known competing financial interests or personal relationships that could have appeared to influence the work reported in this paper.

Acknowledgements

JRS would like to thank Jacqueline Grebmeier and Lee Cooper for help with collecting the samples during HLY2202, as well as the captain and crew of USCGC Healy. JRS would also like to thank the IASC Marine Working Group for travel support. Anja Pappert and the FÖJs and student assistants, who assisted with measuring environmental parameters, are also gratefully acknowledged. Finally, we thank two anonymous reviewers for helpful comments.

Appendix A. Supplementary data

Supplementary data to this article can be found online at https://doi.org/10.1016/j.dsr.2025.104513.

References

Alldredge, A.L., Silver, M.W., 1988. Characteristics, dynamics and significance of marine snow. Prog. Oceanogr. 20, 41–82. https://doi.org/10.1016/0079-6611(88)90053-5.

Aller, R.C., 1994. Bioturbation and remineralization of sedimentary organic matter: effects of redox oscillation. Chem. Geol. 114, 331–345. https://doi.org/10.1016/0009-2541(94)90062-0.

Ambrose, W.G., Renaud, P.E., 1997. Does a pulsed food supply to the benthos affect polychaete recruitment patterns in the Northeast Water Polynya? J. Mar. Syst. 10, 483–495. https://doi.org/10.1016/S0924-7963(96)00053-X.

Anderson, T.R., Rice, T., 2006. Deserts on the sea floor: edward Forbes and his azoic hypothesis for a lifeless deep ocean. Endeavour 30, 131–137. https://doi.org/10.1016/j.endeavour.2006.10.003.

Andrássy, I., 1956. Die Rauminhalts- und Gewichtsbestimmung der Fadenwürmer (Nematoden). Acta Zool. 1–15.

Ansari, K.G.M.T., Lyla, S., Khan, S.A., Bhadury, P., 2017. Trophic diversity, size and biomass spectrum of Bay of Bengal nematodes: a study case on depth and latitudinal patterns. Cont. Shelf Res. 148, 139–149. https://doi.org/10.1016/j.csr.2017.08.018.

Ashjian, C.J., Grebmeier, J.M., 2024. Cruise Report USCGC Healy HLY2202/AWS2022 Synoptic Arctic Survey (SAS) Cruise (Cruise Report).

Azam, F., Malfatti, F., 2007. Microbial structuring of marine ecosystems. Nat. Rev. Microbiol. 5, 782–791. https://doi.org/10.1038/nrmicro1747.

Børsheim, K.Y., Bratbak, G., Heldal, M., 1990. Enumeration and biomass estimation of planktonic bacteria and viruses by transmission electron microscopy. Appl. Environ. Microbiol. 56, 352–356. https://doi.org/10.1128/aem.56.2.352-356.1990.

Clough, L.M., Renaud, P.E., Ambrose Jr., W.G., 2005. Impacts of water depth, sediment pigment concentration, and benthic macrofaunal biomass on sediment oxygen demand in the western Arctic Ocean. Can. J. Fish. Aquat. Sci. 62, 1756–1765. https://doi.org/10.1139/f05-102.

Constable, A.J., Harper, S., Dawson, J., Holsman, K., Mustonen, T., Piepenburg, D., Rost, B., 2022. Cross-chapter paper 6: polar regions. In: Pörtner, H.-O., Roberts, D.C., Tignor, M., Poloczanska, E.S., Mintenbeck, K., Alegria, A., Craig, M., Langsdorf, S., Löschke, S., Möller, V., Okem, A., Rama, B. (Eds.), Climate Change 2022: Impacts, Adaptation and Vulnerability., Contribution of the Working Group II to the Sixth Assessment Report of the Intergovernmental Panel on Climate Change. Cambridge University Press, Cambridge, UK and New York, NY, USA, pp. 2319–2368.

Coull, B.C., 1988. Chapter 3: ecology of the marine meiofauna. In: Thiel, H., Higgins, R.P. (Eds.), Introduction to the Study of Meiofauna. Smithsonian Institution Press, Washington D.C, London, pp. 18–38.
Findlay, R.H., King, G.M., Watling, L., 1989. Efficacy of phospholipid analysis in determining microbial biomass in sediments. Appl. Environ. Microbiol. 55, 2888–2893. https://doi.org/10.1128/aem.55.11.2888-2893.1989.
Fleeger, J.W., Thistle, D., Thiel, H., 1988. Chapter 7: sampling equipment. In: Thiel, H., Higgins, R.P. (Eds.), Introduction to the Study of Meiofauna. Smithsonian Institution Press, Washington D.C, London, pp. 115–125.
Forbes, E., Reeve, L.A., 1855. Literary Papers by the Late Professor Edward Forbes. London, L. Reeve.
Frey, K.E., Comiso, J.C., Cooper, L.W., Garcia-Eidell, C., Grebmeier, J.M., Stock, L.V., 2020. Arctic Ocean primary productivity: the response of marine algae to climate warming and Sea Ice decline. NOAA Tech. Rep. OAR ARC 22. https://doi.org/10.25923/0je1-te61.
Gaffey, C.B., Frey, K.E., Cooper, L.W., Grebmeier, J.M., 2022. Phytoplankton bloom stages estimated from chlorophyll pigment proportions suggest delayed summer production in low sea ice years in the northern Bering Sea. PLoS One 17, e0267586. https://doi.org/10.1371/journal.pone.0267586.
Gerlach, S.A., 1971. On the importance of marine meiofauna for benthos communities. Oecologia 6, 176–190. https://doi.org/10.1007/BF00345719.
Giere, O., 2009. Meiobenthology. The Microscopic Motile Fauna of Aquatic Sediments, second ed. Springer, Berlin, Heidelberg. https://doi.org/10.1007/978-3-540-68661-3.
Giere, O., Eleftheriou, A., Murison, D.J., 1988. Chapter 5: abiotic factors. In: Thiel, H., Higgins, R.P. (Eds.), Introduction to the Study of Meiofauna. Smithsonian Institution Press, Washington D.C, London, pp. 61–78.
Giere, O., Schratzberger, M. (Eds.), 2023. New Horizons in Meiobenthos Research. Profiles, Patterns and Potentials, first ed. Springer, Cham. https://doi.org/10.1007/978-3-031-21622-0.
Graversen, R.G., Mauritsen, T., Tjernström, M., Källén, E., Svensson, G., 2008. Vertical structure of recent Arctic warming. Nature 451, 53–56. https://doi.org/10.1038/nature06502.
Grebmeier, J.M., 2012. Shifting patterns of life in the Pacific Arctic and sub-Arctic seas. Ann. Rev. Mar. Sci 4, 63–78. https://doi.org/10.1146/annurev-marine-120710-100926.
Grebmeier, J.M., Barry, J.P., 1991. The influence of oceanographic processes on pelagic-benthic coupling in polar regions: a benthic perspective. J. Mar. Syst. 2, 495–518. https://doi.org/10.1016/0924-7963(91)90049-Z.
Grebmeier, J.M., Overland, J.E., Moore, S.E., Farley, E.V., Carmack, E.C., Cooper, L.W., Frey, K.E., Helle, J.H., McLaughlin, F.A., McNutt, S.L., 2006. A major ecosystem shift in the northern Bering Sea. Science 311, 1461–1464. https://doi.org/10.1126/science.1121365.
Greiser, N., Faubel, A., 1988. Chapter 6: biotic factors. In: Higgins, R.P., Thiel, H. (Eds.), Introduction to the Study of Meiofauna. Smithsonian Institution Press, Washington D.C, London.
Grossmann, S., Reichardt, W., 1991. Impact of Arenicola marina on bacteria in intertidal sediments. Mar. Ecol. Prog. Ser. 77, 85–93.
Grzelak, K., Kotwicki, L., Hasemann, C., Soltwedel, T., 2017. Bathymetric patterns in standing stock and diversity of deep-sea nematodes at the long-term ecological research observatory HAUSGARTEN (Fram Strait). J. Mar. Syst. 172, 160–177. https://doi.org/10.1016/j.jmarsys.2017.02.003.
Hasemann, C., 2006. Kleinskalige Heterogenität in der arktischen Tiefsee: Einfluß kleiner Kaltwasser-Schwämme auf die Diversität benthischer Nematoden-Gemeinschaften (phd). Universität Bremen. http://nbn-resolving.de/urn:nbn:de:gbv:46-diss000102987.
Hasemann, C., Mokievsky, V.O., Sablotny, B., Tekman, M.B., Soltwedel, T., 2020. Effects of sediment disturbance on deep-sea nematode communities: results from an in-situ experiment at the arctic LTER observatory HAUSGARTEN. J. Exper. Biol. Ecol. 533. https://doi.org/10.1016/j.jembe.2020.151471.
Heip, C.H.R., Vincx, M., Vranken, G., 1985. The ecology of marine nematodes. Oceanogr. Mar. Biol. 23, 399–498.
Holm-Hansen, O., Lorenzen, C.J., Holmes, R.W., Strickland, J.D.H., 1965. Fluorometric determination of chlorophyll. ICES (Int. Counc. Explor. Sea) J. Mar. Sci. 31, 3–15. https://doi.org/10.1093/icesjms/30.1.3.
Ingels, J., Driessche, P., De Mesel, I., Vanhove, S., Moens, T., Vanreusel, A., 2010. Preferred use of bacteria over phytoplankton by deep-sea nematodes in polar regions. Mar. Ecol. Prog. Ser. 406, 121–133. https://doi.org/10.3354/meps08535.
Ingels, J., Hasemann, C., Soltwedel, T., Vanreusel, A., 2023a. Chapter 9: polar meiofauna—antipoles or parallels? In: Giere, O., Schratzberger, M. (Eds.), New Horizons in Meiobenthos Research. Profiles, Patterns and Potentials. Springer, Cham, pp. 285–328.
Ingels, J., Leduc, D., Zeppilli, D., Vanreusel, A., 2023b. Chapter 8: deep-Sea meiofauna—a world on its own or deeply connected? In: Giere, O., Schratzberger, M. (Eds.), New Horizons in Meiobenthos Research. Profiles, Patterns and Potentials. Springer, Cham, pp. 257–284.
Kaariainen, J.I., Bett, B.J., 2006. Evidence for benthic body size miniaturization in the deep sea. J. Mar. Biol. Assoc. U. K. 86, 1339–1345. https://doi.org/10.1017/S0025315406014366.
Kiesel, J., Bienhold, C., Wenzhöfer, F., Link, H., 2020. Variability in benthic ecosystem functioning in arctic shelf and deep-sea sediments: assessments by benthic oxygen uptake rates and environmental drivers. Front. Mar. Sci. 7. https://doi.org/10.3389/fmars.2020.00426.
Kruskal, J.B., 1964. Multidimensional scaling by optimizing goodness of fit to a nonmetric hypothesis. Psychometrika 29, 1–27. https://doi.org/10.1007/BF02289565.
Kruskal, W.H., Wallis, W.A., 1952. Use of ranks in one-criterion variance analysis. J. Am. Stat. Assoc. 47, 583–621. https://doi.org/10.1080/01621459.1952.10483441.
Lampitt, R.S., 1985. Evidence for the seasonal deposition of detritus to the deep-sea floor and its subsequent resuspension. Deep-Sea Res., Part A 32, 885–897. https://doi.org/10.1016/0198-0149(85)90034-2.
Levin, L.A., Gage, J.D., 1998. Relationships between oxygen, organic matter and the diversity of bathyal macrofauna. Deep Sea Res. Part II Top. Stud. Oceanogr. 45, 129–163. https://doi.org/10.1016/S0967-0645(97)00085-4.
Meyer-Reil, L.-A., 1983. Benthic response to sedimentation events during autumn to spring at a shallow water station in the Western Kiel Bight. Mar. Biol. 77, 247–256. https://doi.org/10.1007/BF00395813.
Middelburg, J.J., 2018. Reviews and syntheses: to the bottom of carbon processing at the seafloor. Biogeosciences 15, 413–427. https://doi.org/10.5194/bg-15-413-2018.
NASA Scientific Visualization Studio, 2016. Annual Arctic Sea Ice Minimum 1979-2015 with Area Graph [WWW Document]. NASA Scientific Visualization Studio. URL. https://svs.gsfc.nasa.gov/4435/ (accessed 12.14.23).
National Snow and Ice Data Center, 2022. Ain't no sunshine when she's gone. Arctic Sea Ice News & Analysis [WWW Document]. https://nsidc.org/arcticseaicenews/2022/. (Accessed 8 December 2023).
Paasche, Ø., Olsen, A., Årthun, M., Anderson, L.G., Wängberg, S.-Å., Ashjian, C.J., Grebmeier, J.M., Kikuchi, T., Nishino, S., Yasunaka, S., Kang, S.-H., Cho, K.-H., Azetsu-Scott, K., Williams, W.J., Carmack, E., Torres-Valdés, S., Tyrrell, T., Edelvang, K., He, J., Kassen, H.M., 2019. Addressing arctic challenges requires a synoptic ocean Survey. Eos 100. https://doi.org/10.1029/2019EO136200.
Paulus, E., 2021. Shedding light on deep-sea biodiversity—a highly vulnerable habitat in the face of anthropogenic change. Front. Mar. Sci. 8. https://doi.org/10.3389/fmars.2021.667048.
Piepenburg, D., 2005. Recent research on Arctic benthos: common notions need to be revised. Polar Biol. 28, 733–755. https://doi.org/10.1007/s00300-005-0013-5.
Platt, H.M., Warwick, R.M., 1988. Free living marine nematodes Part II. British Chromadorids, Synopses of the British Fauna. Cambridge University press, for the Linnean Society of London and The Estuarine and Brackish-Water Sciences Association, New York, København, Köln.
Previdi, M., Smith, K.L., Polvani, L.M., 2021. Arctic amplification of climate change: a review of underlying mechanisms. Environ. Res. Lett. 16, 093003. https://doi.org/10.1088/1748-9326/ac1c29.
Przeslawski, R., 2020. Lebensspuren – more than just a fancy word for deep-sea poo. Schmidt Ocean Institute. URL. https://schmidtocean.org/cruise-log-post/lebensspuren-more-than-a-fancy-word/ (accessed 1.16.24).
R Core Team, 2023. R: A Language and Environment for Statistical Computing.
Renaud, P.E., Ambrose, W.G., Vanreusel, A., Clough, L.M., 2006. Nematode and macrofaunal diversity in central Arctic Ocean benthos. J. Exper. Marine Biol. Ecol.A Tribute to Richard M. Warwick 330, 297–306. https://doi.org/10.1016/j.jembe.2005.12.035.
Rogers, A., 2015. Environmental change in the deep ocean. Annu. Rev. Environ. Resour. 40, 1–38. https://doi.org/10.1146/annurev-environ-102014-021415.
Rosli, N., Leduc, D., Rowden, A.A., Probert, P.K., 2018. Review of recent trends in ecological studies of deep-sea meiofauna, with focus on patterns and processes at small to regional spatial scales. Mar. Biodivers. 48, 13–34. https://doi.org/10.1007/s12526-017-0801-5.
Rudels, B., Carmack, E., 2022. Arctic Ocean water mass structure and circulation. Oceanography (Wash. D. C.) 35, 52–65. https://doi.org/10.5670/oceanog.2022.116.
Schewe, I., 2001. Small-sized benthic organisms of the alpha ridge, central Arctic Ocean. Int. Rev. Hydrobiol. 86, 317–335. https://doi.org/10.1002/1522-2632(200106)86:3<317::AID-IROH317>3.0.CO;2-V.
Schewe, I., Soltwedel, T., 1999. Deep-sea meiobenthos of the central Arctic Ocean: distribution patterns and size-structure under extreme oligotrophic conditions. Vie et milieu, Life Environ. 49, 79–92.
Schnier, J., Hasemann, C., Mokievsky, V., Martínez Arbizu, P., Soltwedel, T., 2023. Nematode communities along a bathymetric transect in the deep eastern Fram Strait (Arctic Ocean): interrelations between diversity, function and environment. Front. Mar. Sci. 10. https://doi.org/10.3389/fmars.2023.1271447.
Schratzberger, M., Ingels, J., 2018. Meiofauna matters: the roles of meiofauna in benthic ecosystems. In: Journal of Experimental Marine Biology and Ecology, IçIMCo, the 16th International Meiofauna Conference, 502, pp. 12–25. https://doi.org/10.1016/j.jembe.2017.01.007.
Schratzberger, M., Larcombe, P., 2014. The role of the sedimentary regime in shaping the distribution of subtidal sandbank environments and the associated meiofaunal nematode communities: an example from the southern North sea. PLoS One 9, e109445. https://doi.org/10.1371/journal.pone.0109445.
Seinhorst, J.W., 1962. On the killing, fixation and transferring to glycerin of nematodes. Nematologica 8, 29–32. https://doi.org/10.1163/187529262X00981.
Seinhorst, J.W., 1959. A rapid method for the transfer of nematodes from fixative to anhydrous glycerin. Nematologica 4, 67–69. https://doi.org/10.1163/187529259X00381.
Smith, C.R., Demopoulos, A., 2004. The deep pacific ocean floor. In: Tyler, P.A. (Ed.), Ecosystems of the Deep Oceans. Ecosystems of the World. Elsevier, Amsterdam, pp. 179–218.
Snelgrove, P.V.R., Butman, C.A., 1994. Animal sediment relationships revisited – cause versus effect. Oceanogr. Mar. Biol. 32.
Soetaert, K., Muthumbi, A., Heip, C., 2002. Size and shape of ocean margin nematodes: morphological diversity and depth-related patterns. Mar. Ecol. Prog. Ser. 242, 179–193. https://doi.org/10.3354/meps242179.

Soetaert, K.E.R., Heip, C.H.R., 1995. Nematode assemblages of deep-sea and shelf break sites in the North-atlantic and mediterranean-sea. Mar. Ecol. Prog. Ser. 125, 171–183. https://doi.org/10.3354/meps125171.

Soltwedel, T., 2000. Metazoan meiobenthos along continental margins: a review. Prog. Oceanogr. 46, 59–84. https://doi.org/10.1016/S0079-6611(00)00030-6.

Soltwedel, T., Bauerfeind, E., Bergmann, M., Bracher, A., Budaeva, N., Busch, K., Cherkasheva, A., Fahl, K., Grzelak, K., Hasemann, C., Jacob, M., Kraft, A., Lalande, C., Metfies, K., Nöthig, E.-M., Meyer, K., Quéric, N.-V., Schewe, I., Włodarska-Kowalczuk, M., Klages, M., 2016. Natural variability or anthropogenically-induced variation? Insights from 15 years of multidisciplinary observations at the arctic marine LTER site HAUSGARTEN. Ecol. Indicators, Value Long-Term Ecosys. Res. (LTER): Address Global Change Ecol. Site-Based Data 65, 89–102. https://doi.org/10.1016/j.ecolind.2015.10.001.

Soltwedel, T., Bauerfeind, E., Bergmann, M., Budaeva, N., Hoste, E., Jaeckisch, N., Von Juterzenka, K., Matthiesson, J., Moekievsky, V., Nöthig, E.-M., Quéric, N.-V., Sablotny, B., Sauter, E., Schewe, I., Urban-Malinga, B., Wegner, J., Maria Wlodarska-Kowalczuk, M., Klages, M., 2005. HAUSGARTEN: multidisciplinary investigations at a deep-sea, long-term observatory in the Arctic Ocean. Oceanography (Wash. D. C.) 18, 46–61. https://doi.org/10.5670/oceanog.2005.24.

Soltwedel, T., Grzelak, K., Hasemann, C., 2020. Spatial and temporal variation in deep-sea meiofauna at the LTER observatory HAUSGARTEN in the Fram Strait (Arctic Ocean). Diversity 12, 279. https://doi.org/10.3390/d12070279.

Soltwedel, T., Guilini, K., Sauter, E., Schewe, I., Hasemann, C., 2018. Local effects of large food-falls on nematode diversity at an arctic deep-sea site: results from an *in situ* experiment at the deep-sea observatory HAUSGARTEN. In: Journal of Experimental Marine Biology and Ecology, IçIMCo, the 16th International Meiofauna Conference, 502, pp. 129–141. https://doi.org/10.1016/j.jembe.2017.03.002.

Soltwedel, T., Pfannkuche, O., Thiel, H., 1996. The size structure of deep-sea meiobenthos in the North-Eastern Atlantic: nematode size spectra in relation to environmental variables. J. Mar. Biol. Assoc. U. K. 76, 327–344.

Soltwedel, T., Schewe, I., 1998. Activity and biomass of small benthic biota in the central Arctic Ocean. Polar Biol. 19 (1), 52–62. https://doi.org/10.1007/s003000050215. Supplement to: Soltwedel, T; Schewe, I (1998): Activity and biomass of the small benthic biota in the Central Arctic Ocean.

Soltwedel, T., Schewe, I., 1997. Activity and biomass of the small benthic biota in the Central Arctic Ocean. Polar Biol. 19, 52–62. https://doi.org/10.1007/s003000050215.

Suess, E., 1980. Particulate organic carbon flux in the oceans—surface productivity and oxygen utilization. Nature 288, 260–263. https://doi.org/10.1038/288260a0.

Thiel, H., 1983. Meiobenthos and nanobenthos of the deep-sea. In: Rowe, G.T. (Ed.), Deep Sea Biology. The Sea. John Wiley and Sons, New York, pp. 167–230.

Thiel, H., 1978. Benthos in upwelling regions. In: Boje, R., Tomczak, M. (Eds.), Upwelling Ecosystems. Springer, Berlin, Heidelberg, pp. 124–138. https://doi.org/10.1007/978-3-642-66985-9_11.

Thiel, H., 1975. The size structure of the deep-sea benthos. Int. Rev. Gesamten Hydrobiol. 60, 575–606.

Thistle, D., 1978. Harpacticoid dispersion patterns: implications for deep-sea diversity maintenance. J. Mar. Res. 36, 377–297.

Tietjen, J.H., 1992. Abundance and biomass of metazoan meiobenthos in the Deep Sea. In: Rowe, G.T., Pariente, V. (Eds.), Deep-Sea Food Chains and the Global Carbon Cycle, NATO ASI Series. Springer, Netherlands, Dordrecht, pp. 45–62. https://doi.org/10.1007/978-94-011-2452-2_4.

Tita, G., Vincx, M., Desrosiers, G., 1999. Size spectra, body width and morphotypes of intertidal nematode: an ecological interpretation. J. Marine Biol. Assoc. UK 79, 1007–1015. https://doi.org/10.1017/S0025315499001241.

Udalov, A., Azovsky, A., Mokievsky, V., 2005. Depth-related pattern in nematode size: what does the depth itself really mean? Prog. Oceanogr. 67, 1–23. https://doi.org/10.1016/j.pocean.2005.02.020.

Vanaverbeke, J., Steyaert, M., Vanreusel, A., Vincx, M., 2003. Nematode biomass spectra as descriptors of functional changes due to human and natural impact. Mar. Ecol. Prog. Ser. 249, 157–170. https://doi.org/10.3354/meps249157.

Vanreusel, A., Clough, L., Jacobsen, K., Ambrose, W., Jutamas, Jivaluk, Ryheul, V., Herman, R., Vincx, M., 2000. Meiobenthos of the central Arctic Ocean with special emphasis on the nematode community structure. Deep Sea Res. Oceanogr. Res. Pap. 47, 1855–1879. https://doi.org/10.1016/S0967-0637(00)00007-8.

Vanreusel, A., Martínez Arbizu, P., Yasuhara, M., 2023. Chapter 5: marine meiofauna diversity and biogeography—paradigms and challenges. In: Schratzberger, M., Giere, O. (Eds.), New Horizons in Meiobenthos Research. Springer, pp. 121–151.

Vincx, M., 1996. Chapter 15: meiofauna in marine and fresh water sediments. In: Hall, G. S. (Ed.), Methods for the Examination of Organismal Diversity in Soils and Sediments. CAB International, pp. 214–248.

Wieser, W., 1960. Benthic studies in buzzards bay Ii. The meiofauna. Limnol. Oceanogr. 5, 121–137. https://doi.org/10.4319/lo.1960.5.2.0121.

Wieser, W., 1959. The effect of grain size on the distribution of small invertebrates inhabiting the beaches of puget sound. Limnol. Oceanogr. 4, 181–194. https://doi.org/10.4319/lo.1959.4.2.0181.

Wigley, R.L., McIntyre, A.d., 1964. Some quantitative comparisons of offshore meiobenthos and macrobenthos south of martha's vineyard. Limnol. Oceanogr. 9, 485–493. https://doi.org/10.4319/lo.1964.9.4.0485.

Yentsch, C.S., Menzel, D.W., 1963. A method for the determination of phytoplankton chlorophyll and phaeophytin by fluorescence. Deep Sea Res. Oceanogr. Abstr. 10, 221–231. https://doi.org/10.1016/0011-7471(63)90358-9.

Zhulay, I., Iken, K., Renaud, P.E., Kosobokova, K., Bluhm, B.A., 2023. Reduced efficiency of pelagic–benthic coupling in the Arctic deep sea during lower ice cover. Sci. Rep. 13, 6739. https://doi.org/10.1038/s41598-023-33854-0.